Evaluation of the Effects of Hyperbaric Dive Environments on the Autonomic Nervous System Using Principal Dynamic Mode Analysis

by
Yan Bai

A Dissertation
Submitted to the Faculty
of the
WORCESTER POLYTECHNIC INSTITUTE
in partial fulfillment of the requirements for the
Degree of Doctor of Philosophy
in
Biomedical Engineering
August 2011

APPROVED:

Dr. Ki H. Chon, Advisor, Committee Chair, Head of Department

Dr. Yitzhak Mendelson, Committee Member

Dr. Domhnull Granquist-Fraser, Committee Member

Dr. Soussan Djamasbi, Committee Member

Dr. Joe White, Committee Member
State University of New York at Stony Brook

Evaluation of the Effects of Hyperbaric Dive Environments on the Autonomic Nervous System Using Principal Dynamic Mode Analysis

by
Yan Bai

A Dissertation
Submitted to the Faculty
of the
WORCESTER POLYTECHNIC INSTITUTE
in partial fulfillment of the requirements for the
Degree of Doctor of Philosophy
in
Biomedical Engineering
August 2011

Approved by:

Ki H. Chon, PhD
Professor, Head of Department
Department of Biomedical Engineering
Worcester Polytechnic Institute

Yitzhak Mendelson, PhD
Associate Professor
Department of Biomedical Engineering
Worcester Polytechnic Institute

Domhnull Granquist-Fraser, PhD
Assistant Professor
Department of Biomedical Engineering
Worcester Polytechnic Institute

Soussan Djamasbi, PhD
Associate Professor
School of Business
Worcester Polytechnic Institute

Joseph C. White, MD
Professor
Department of Family Medicine
State University of New York at Stony Brook

Abstract

As water covers over 75% surface area of the earth, humans have an innate desire to explore the underwater environment for various aims. Physiological responses are induced in humans and animals to adapt to different stresses imposed by the hyperbaric environment. When these stresses become overwhelming, certain hazards can occur to individuals in underwater or in similar hyperbaric environments, and they may include nitrogen narcosis, oxygen toxicity and decompression sickness (DCS). There are evidences showing that the autonomic nervous system (ANS) plays an important role in diving reflex and physiological responses to diving hazards. However, the assessment of the autonomic nervous activity during SCUBA dives and diving-related hazards are mostly absent from the literature. Thus, in order to evaluate the autonomic nervous alterations that may occur during diving, especially during DCS, the following three experiments were performed in this study: the simulated dives of human subjects in a hyperbaric chamber, the SCUBA diving performed in seawater and induced DCS in a swine model. A novel algorithm developed in our lab, principal dynamic mode (PDM) analysis, is applied to the above data. It has been shown that the PDM is able to accurately separate the sympathetic and parasympathetic dynamics of the ANS, and subsequently it is able to obtain a better quantification of the autonomic nervous activity than a current golden-standard approach. Through the study, dominance of the parasympathetic modulation was found in both hyperbaric chamber and SCUBA diving conditions. And more stresses were present in real dives, compared to simulated dives in chamber. In the swine DCS model, we found neurological DCS and cardiopulmonary DCS resulted in different alterations in the ANS. Furthermore, tracking dynamics of the parasympathetic modulations via the PDM method may allow discrimination between cardiopulmonary DCS and neurological DCS, and has potential use as a marker for early diagnosis of cardiopulmonary DCS.

Acknowledgements

I would like to thank my advisor, Dr. Ki Chon, for the exciting topics suggested, for interesting discussions and for his guidance and continuous support.

I would like to thank Dr. Peter Brink and Dr. Joe White, who coordinated all the human diving experiments.

I would like to thank all divers that participated in this study.

I would like to thank Wayne Koller and Richard Mahon, who performed swine experiments in this study.

I would like to thank all my labmates for all their support and help. They are Xinnian Chen, Jinsoek Lee, Sheng Lu, Chris Scully, King Lung Siu, Nandakumar Selvaraj, Biin Song, Bufan Yang, He Zhao and Yuru Zhong.

I would like to thank my families, my wife and my parents, for their long-term support and encouragement.

Table of Contents

List of Tables

List of Figures

Glossary

Approximate Entropy (ApEn): a quantitative measure of the complexity of a given system derived from information theory.

Atmosphere Absolute (ATA): the total pressure exerted on an object, by a gas or mixture of gases, at a specific depth or elevation, including normal atmospheric pressure. 1 ATA of pressure is equivalent to the pressure exerted by around 33 ft of salt water.

Autonomics Nervous System (ANS): the part of the peripheral nervous system that acts as a control system functioning largely below the level of consciousness, and controls visceral functions.

Cardiopulmonary Decompression Sickness (CP DCS): a special decompression sickness condition as a result of massive bubbles entering pulmonary arterial circulation and featured with symptoms of deep chest pain and dyspnea.

Cutis Marmorata (cutis): refers to mottled or marbled skin usually around the shoulders, upper chest and abdomen, with itching in decompression sickness. It happens when bubbles form in cutaneous system.

Decompression Sickness (DCS): a disease arising from dissolved gases coming out of tissues into bubbles inside the body during decrease of pressure.

Feet under Sea Water (fsw): a unit of pressure which measures pressure by the depth underwater.

Jacketed External Telemetry (JET): a telemetry system developed by Data Sciences International to monitor non-invasive ECG for large animals. We used it to record ECG in swine experiments.

Low Frequency (LF): the frequency band between 0.04-0.15 Hz in the power spectrum of heart rate variability in human. It is controlled by both the sympathetic and parasympathetic systems.

High Frequency (HF): the frequency band between 0.15-0.4 Hz in the power spectrum of heart rate variability in human. It is controlled mainly by the parasympathetic system.

Hear rate variability (HRV): a physiological phenomenon where the time interval between heart beats varies. This variability can be captured and quantified to measure the function of the autonomic nervous system.

Muscle Sympathetic Nerve Activity (MSNA): the electrical activity of the sympathetic nerves in muscle. It can be measured invasively by certain electrodes, and be quantified by burst amplitude and frequency of recorded nerve impulses.

Parasympathetic Nervous System: one of the two main divisions of the autonomic nervous system. The parasympathetic system specifically is responsible for stimulation of "rest-and-digest" activities that occur when the body is at rest, including sexual arousal, salivation, lacrimation (tears), urination, digestion and defecation.

Power Spectral Density (PSD): the strength of the variations (energy) as a function of frequency associated with a stationary stochastic process, or a deterministic function of time.

Principal Dynamic Mode (PDM): a non-linear mathematical method to extract only the principle components within a signal via eigen decomposition.

RMSSD: the root-mean square of the successive difference of R-R intervals, associated with the parasympathetic modulation.

SCUBA Diving: a form of underwater diving in which a diver uses a set of self contained underwater breathing apparatus (SCUBA) to breathe underwater.

SDNN: standard deviation of R-R intervals from successive 5-minute periods, reflecting overall activity of the autonomic nervous system.

Sympathetic Nervous System: one of the two main divisions of the autonomic nervous system. Its general action is to mobilize the body's resources under stress; to induce the fight-or-flight response. It is thought counteract the parasympathetic system.

Introduction

Ancient humans began breath-hold diving, maybe for the aim of gathering food or just simply exploring the underwater environment. Even today, a large number of professional divers still perform this traditional diving method off the Pacific coasts to collect pearls and sponges. Some others developed breath-holding diving into a competitive sport, referred as apnea diving. About hundreds of years ago, diving bell and early diving suit were invented, but they still need an umbilical cord to supply air from the surface. Only until last century, the development of the self contained underwater breathing apparatus (SCUBA) provided diving with great flexibility and even made it become a very popular recreational activity. This device contains a high pressure air tank that can be carried by a diver, and the diver breathes air through a mouthpiece which is connected to the tank with a two stage demand valve system. It is estimated that approximately 7 million divers are active worldwide and 500,000 new divers are training annually (30). Many professionals actively carry out diving for the purposes of seafood harvesting, research, construction, salvage and military.

Due to their similarity in nature, exposures to hyperbaric ambient other than underwater environment are also referred as dive in many occasions, as well as in this dissertation. Examples of such dives include hyperbaric O_2 therapy (56), simulated dives for hyperbaric research, and working in a compressed atmosphere for construction of tunnels or caissons. Additionally, in some commercial activities requiring deep dives for many days, divers are usually first compressed in a large chamber or habitat to a pressure which is similar to the pressure at their working depth, then live in it for subsequent dives. They are transported to the working site by a pressurized diving bell. In this way, divers can continue working at depth for a period from several days to several weeks without frequent decompressions. Staying at high pressure for such a long time makes gases dissolved in divers' body tissues reach equilibrium and saturate the tissues, so this kind of diving is usually referred as saturation diving.

Hyperbaric environments may also result from catastrophic accidents at sea or underground (42). For examples, survivors may stay at high pressure for several days and get saturated while waiting for rescue in a disabled submarine (DISSUB). It is very possible for them to encounter decompression sickness (DCS) since rescue effort may not

allow a slow, controlled decompression. Though submarine accidents seldom happen, the sinking of Russian submarine Kursk in 2000 reminds us to prepare for such scenarios. Currently the US Navy has agreements for assistance of DISSUB rescue with >20 countries (17). Our aim is to understand physiological changes that occur during diving and in diving related hazardous conditions, and to find if there is any method that can predict or avoid these hazardous conditions including the DCS.

Diving Physiology and Decompression Sickness

Individuals encounter many stresses in the underwater environment, including high ambient pressure, breathing gases of high density, increased resistance to movement, additional weight of diving equipment, cold water, low visual ability and a high breathing resistance. Human body automatically makes physiological responses to adapt to this unusual environment. Diving equipments and standard diving procedures also help to minimize these stresses. However, failure to deal with these stresses properly may bring unexpected hazards and even fatal events to divers.

When the body is immersed into water, especially when the face is immersed, the diving response, also called diving reflex, is induced through the trigeminal nerve on the face (19, 22). It is first featured with a reduction in the heart rate (a bradycardia) as a result of increased vagal activity. There is also an increase in arterial blood pressure due to peripheral vasoconstriction resulting from increased sympathetic activity. Above process is actually a redistribution of body blood, as the peripheral blood flows into the central circulation. It causes the increase in heart volume, stroke volume and cardiac output. The benefit of diving response is to conserve heat and provide oxygen primarily to vital organs, like the brain and heart. Breath holding, cold water and increased oxygen partial pressure are all believe to improve the magnitude of diving reflex. Additionally, the hydrostatic pressure of the surrounding water balances the hydrostatic pressure within the systemic circulation, and shifts the blood from the vein of the lower part of body to the central circulation (19). Thus, this effect also increases the cardiac output and reduces the heart rate. These conditions also exist in dry hyperbaric environment, where diving response is not induced. Another effect of vasoconstriction is to induce the release of antidiuretic hormone and result in diuresis.

As ambient pressure increases, divers first encounter an increase of breathing gas density. This brings reduced pulmonary compliance, increased airways resistance and work of breathing. All these increase the burden on divers (19). Furthermore, the partial pressure of each gas component in the divers' breathing gas increases proportionally, as the pressure of breathing gas itself increases (Dalton's Law). Exposure to gases with high partial pressure proportionally increases the amount of these gases that are dissolved in body tissues (Henry's Law), until the amount dissolved reaches equilibrium (30). These supra-normal quantities of gases in tissues can impair the function of the neural systems, damage body tissues and cause the problems of O_2 toxicity, N_2 narcosis and high-pressure nervous syndrome (16). In practice, divers use different gas mixtures and add inert gases (H_2 and He) into breathing gas to avoid above described problems, but no method can guarantee 100 percent safety since all diving gases actually have potential toxic effects.

During ascent, the dissolved gases are released as the ambient pressure decreases. However, for a quick ascent without proper decompression stops, these gases can form a lot of bubbles in blood and tissues. When the amount of bubbles exceeds the ability of human body to diffuse them, the syndrome of decompression sickness appears (53, 55). There are on average 1100 cases of DCS annually reported in US alone (3). Divers Alert Network (DAN), located at Duke University, prospectively collects dive profiles since 1995, mainly in North America. Their cumulative data includes 135,546 dives by more than 11,000 divers as reported in 2006 (4). It is estimated that the incidence of decompression illness is 0.035% of dives, or 0.43% of divers, based on these data. Dive tables are recommended to minimize the probability of DCS, which define decompression procedures for certain dive profiles (duration, depth and breathing gas). Although these tables are conservative, they cannot guarantee a safety due to the individual variability of susceptibility to DCS. An incidence of 0.003% of DCS has been reported, even when the dive profile seems to have no obvious risk (5).

Table 1 Incidence of different symptoms of decompression illness (53)

Symptoms	*Occurrence as First Symptom (%)*	*Total Occurrence (%)*
Neurologic		
Severe		
Unconsciousness	2.1	4.2
Paralysis	0.7	5.7
Visual disturbance	0.0	6.4
Difficulty walking	0.5	10.6
Semiconscious	0.5	3.4
Bowel control problem	0.0	1.6
Speech disturbance	0.4	2.8
Bladder control problem	0.0	3.0
Convulsion	0.2	0.4
Mild/Ambiguous		
Numbness	21.7	83.4
Dizziness	8.3	23.7
Decreased skin sensation	0.5	10.8
Personality change	0.2	3.2
Reflex change	0.0	1.2
Weakness	5.5	25.8
Neurologic Total	40.6	81.3
Cardiorespiratory	1.8	4.1
Pain/Skin/Nonspecific Symptoms		
Pain	33.9	78.4
Extreme fatigue	5.5	20.8
Headache	8.1	22.6
Nausea	3.4	15.9
Pruritus	2.7	8.3
Rash	0.7	4.4
Restlessness	0.4	4.1
Muscles twitch	0.4	3.5
Hemoptysis	0.4	0.7
Pain/Skin/Nonspecific Total	55.3	12.7
Ambiguous (also possibly due to barotrauma)		
Hearing loss	0.0	1.1
Tinnitus	0.2	3.4
Other	2.4	6.2

It is a popular hypothesis that bubbles are developed around gas micronuclei already existing in body tissues (19, 55). Since oxygen actively participates in metabolism, they are essentially formed by inert gases, mostly nitrogen. Bubbles are mainly found in venous circulation and tissues have different dissolving rate of nitrogen with surrounding tissues, like joints and fat. They also enter arteries if not fully diffused in lung circulation. In the extravascular space, as bubbles increase in size or coalesce, they distort tissues and

nerve endings, thus produce pain and even damage tissues (53). Intravascular bubbles damage both luminal surfactant layer and endothelial cells (30). They may denature proteins, aggregate platelets and red blood cells, activate the complement system and leucocytes, and initiate the coagulation cascade (53). They may also block blood supply to tissues and cause tissue ischemia. When enough bubbles are present, gross hemodynamic abnormalities and cardiovascular alterations can be induced.

DCS is usually divided into Type I and Type II based on the symptoms. Type I DCS affects musculoskeletal or cutaneous system, referred as "the bends". Its symptoms include skin itching, formication, mottled or marbled skin, pain in joint/muscle, and lymph node swelling (53, 55). Musculoskeletal pain is a very common feature of DCS. For example, joint pain appears in 80% of all DCS cases (Table 1). The pain is often vague and diffuse, ranging from superficial to deep. The most susceptible body parts to the pain are the upper extremities. The shoulder is the most common site, followed by the elbows and arms in turn by other body parts. It is believed that tendon sheaths or joint capsules may be irritated mechanically by gas bubbles that form in these tissue compartments. Generally, Type I DCS is not life threatening, but it could be the preceding sign of more severe DCS.

Type II DCS is much more severe than Type I, which is characterized by vestibular, cardiopulmonary or neurological manifestations. Type I and II DCS actually may appear at the same time, which makes this tradition classification appear to be inaccurate. 48% of divers classified as Type I also reported neurological symptoms according to DAN (3). When bubbles form in inner ear, vestibular DCS presents with the symptoms of loss of balance, vertigo, hearing loss or nausea. Cardiopulmonary DCS, "the chokes", is a result of massive bubbles entering pulmonary arterial circulation and featured with symptoms of deep chest pain and dyspnea (53). It rarely happens, but it can cause respiratory failure and is life threatening. Neurological symptoms are more frequent than the other two. They eventually develop in 80% of all DCS cases (Table 1), although they may not appear at the beginning of DCS. These symptoms can be further divided into two categories. Cerebral symptoms, which involve bubbles formed in the brain, include headaches, vision loss, gait disturbance, fatigue and seizure. Spinal cord injury is most commonly involved in neurological DCS. Its symptoms include sensory problems

(numbness, tingling and paresthesia), low back pain, abdominal pain, loss of bowel/bladder control, lower extremity weakness or paralysis (40). The pathophysiology of spinal cord injury involves extravascular bubble growth in spinal white matter (20), the thrombogenetic effect of venous gas bubbles in the epidural venous plexus surrounding the spinal cord, and its subsequent effects of venous drainage obstruction and spinal cord ischemia (21).

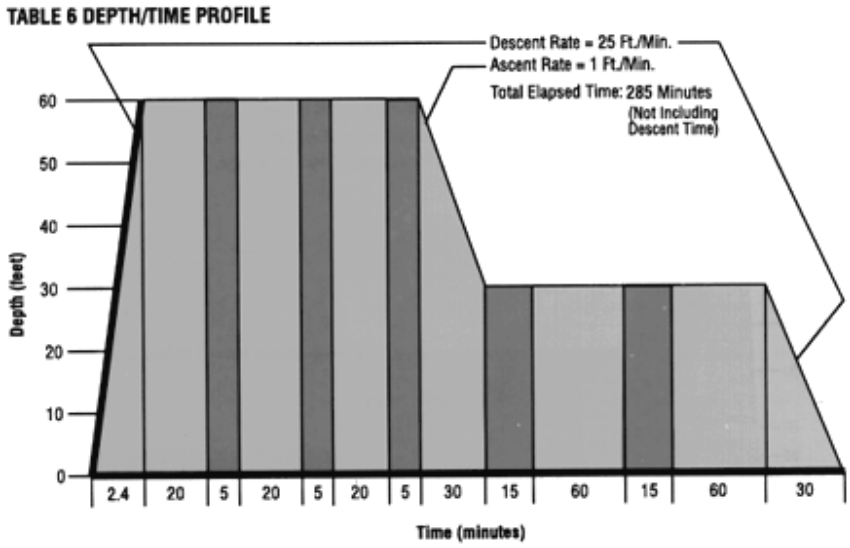

Figure 1. US Navy Table 6 for treatment of DCS. Light shaded areas represent periods of breathing 100% FiO_2; dark shaded areas periods of air break.

The onset of DCS usually occurs within a short period after a dive; 42% of DCS occurs within one hour, 60% within three hours, 83% within eight hours and 98% occurs within 24 hours (1). Long duration, deep depth and rapid or multiple ascents all increase the incidence of DCS. Except these, individual risk factors of DCS include age, obesity, dehydration, gender (female is more susceptible), cold and patent foramen ovale (12, 57). The most effective treatment of DCS is the immediate recompression. This is performed by placement of subjects in hyperbaric chamber with a pressure of two to three atmospheres absolute (ATA) while breathing 100% oxygen, which helps to eliminate inert gas in tissues. The treatment profile most commonly used is the US Nave Table 6 (Figure 1). It begins with staying at 60 feet of sea water (2.8 ATA) for a specified period, then the subject is brought up to 30 feet of sea water (fsw) for a longer period, approximately 3 hours. The subject breathes 100% FiO_2 throughout the treatment except for air breaks to avoid oxygen toxicity. During emergency transportation of DCS patients,

high altitude should be avoided, since it may significantly exacerbate the effect of DCS. If recompression facility is not available, breathing 100% oxygen has been proved to be helpful (31).

Autonomic Nervous Activity during Diving

From above introduction, it is known that the autonomic nervous system (ANS) may play an important role in dive related responses. It works actively to help individuals to adapt to the underwater environment. Many studies have been conducted to evaluate the ANS activity during diving (58). However, most of these studies were performed in dry hyperbaric environments or just induced diving response by immersing a face in a basin of water, due to difficulties to carry out real wet dives. The methods to assess the ANS activity include the measurement of muscle sympathetic nerve activity (MSNA) and catecholaminergic transmitter, drug blockade of the ANS and analysis of heart rate variability (HRV). HRV analysis is a very useful non-invasive method to quantify the ANS activity. It involves time series analysis of continuous beat-to-beat heart rate data, in time domain, and also in the frequency domain with the computation of power spectral density (PSD) (2). Specifically, it has been determined for humans that the low frequency band (LF: 0.04-0.15 Hz) in the PSD of heart rate is mediated by both the sympathetic and parasympathetic nervous regulations whereas the high frequency band (HF: 0.15-0.4 Hz) is widely believed to be dominated by the parasympathetic nervous system (including respiratory sinus arrhythmias). The ratio between LF and HF (LF/HF) is usually used to estimate the balance between sympathetic and parasympathetic systems. Thus, HRV analysis has been applied in many studies in which ANS is significantly altered, such as the studies on myocardial infarction (27), hypertension (47), anesthesia (39) and diabetes.

Bradycardia has been observed during exposure in various hyperbaric conditions. High ambient pressure, high gas density and high partial pressure of inert gas were all proposed to contribute to this bradycardia. When human subjects breathing air were exposed to hyperbaric environment around 3 ATA, decreased MSNA (59) and increased HF in PSD of HRV (31) were observed, which indicate the decrease of sympathetic activity and the increase of parasympathetic activity. But another study performed through pharmacological blockade of the ANS, concluded that it is the reduced sympathetic activity that plays a primary role in bradycardia (61). Hyperoxia also

contributes to lower heart rate. Breathing 100% oxygen itself can reduce heart rate and MSNA at normobaric condition (48). In a study performed at sea level, HF power increased progressively as the fraction of oxygen in breathing gas increased (49). Additionally, at 2.5 ATA, there was a further increase of HF while breathing 100% oxygen when compare to breathing air, although heart rate did not change when breathing these two different gases (32). The mechanism of hyperoxic bradycardia is unclear. It could be because of hyperoxia induced peripheral vasoconstriction or the reduced input to peripheral or central chemoreceptors.

Some studies of saturation dive were performed at extreme high ambient pressure. Since this kind of studies usually take many days to avoid rapid changes of pressure, we can observe long term effect of hyperbaric environment on human. Yamzaki et al. found decreased heart rate, increased HF and unchanged LF on the first day at 24 ATA, but these alterations diminished on the following days (60). In another study at 34 ATA, urinary adrenaline, LF and HF both increased at the beginning of bottom time, and they gradually went back to baseline thereafter (28). In the study of Hirayanagi et al. with environmental pressure varying from 30 ATA to 40 ATA, no change of heart rate (HR) and HRV was found during diving, but plasma norepinephrine (NE) was found increased during and after dive (24). Thus, in very high pressure condition, there are divergent results on changes in HRV. In the study by Hirayanagi et al., there was actually also an increase of HF on the first day, though this increase was not significant. Therefore, it is more likely that parasympathetic tone is enhanced in severe hyperbaric environments, but attenuates with the duration of staying at depth. Despite different results of LF alteration, sympathetic activity should increase due to hyperbaric stress, since plasma NE or urinary adrenaline is a more direct measurement of the ANS activity than HRV analysis. Thus, both branches of ANS may work actively at the beginning of dive to adapt to severe high pressure, and then become less active after the adaption to this environment.

There are only a few studies on estimating the ANS activity during wet dives. Schipke and Pelzer studied the HRV changes during immersion (head out), submersion (face immersion) and SCUBA diving in a swimming pool with water temperature of 27 ºC (46). There was a slight increase in LF, and this increase became significant during diving, whereas HF was higher during immersion, submersion and diving than during the

control condition. The ratio of LF/HF significantly decreased during immersion and submersion, but not during diving. Thus, parasympathetic system was already activated during immersion and there was no difference of the ANS tone between immersion and submersion. During diving, peripheral sympathetic activity must increase due to diving reflex and the stimulus of cold water, but the change of cardiac sympathetic activity is not certain. It may increase together with peripheral sympathetic activity, decrease to cause bradycardia or increase due to psychological stress (41) in the underwater environment. The authors concluded that the significant increase of LF in their study is mainly due to the shift of respiratory rate from HF range to LF range during diving, since the dive in swimming pool should not produce much mental stress for professional divers. So there was only a slight increase of sympathetic activity in their study. They also suggested that a reduction of HRV in response to diving implies potential physiological problems to subjects. Chouchou et al. performed HRV analysis during recreational SCUBA diving (15). They observed an increase in HF, as well as a decrease of LF/HF, during free recreational dives about 40 minutes in length. They concluded this as a rise in parasympathetic activity and a decrease in cardiac sympathetic activity, but they did not give the detail data of LF which makes it difficult to evaluate their conclusion regarding the sympathetic activity. Since LF/HF ratio decreased significantly, it is likely that their LF did not increase during diving.

In summary, dry hyperbaric environment with relative low pressure (3 ATA), increases vagal activity and decreases sympathetic activity. During saturation dive at relative high pressure (24-40 ATA), both sympathetic and parasympathetic activities increase due to increased hyperbaric stress, but they may gradually return to baseline level after the beginning of dive. In SCUBA diving, the parasympathetic activity and peripheral sympathetic activity increase. But the cardiac sympathetic activity may be unchanged or even decreased in a shallow or recreational dive. From the results of long-term saturation dive at severe high pressure, we can speculate that, it will finally increase as the diving stress increases (diving depth or duration increases). Assessment of the ANS activity may be helpful to find potential hazards during diving. Furthermore, the effect of DCS on ANS is mostly absent from the literature. Thus, it is an interesting topic to investigate.

Principal Dynamic Mode Analysis

HRV analysis is a reasonable non-invasive approach to determine the state of the ANS modulation. However, from previous studies, we can find that there are conflicting results of HRV analysis during diving, and some results from HRV contradict the results from other methods of assessing the ANS activity. This is mainly because the PSD is a linear technique and cannot capture nonlinear properties of HR control. A plethora of recent studies have shown that the physiological mechanisms responsible for HRV have nonlinear components (2, 62). Additionally, the PSD method cannot separate the dynamics of the two nervous system components since both the sympathetic and parasympathetic nervous regulations operate in the LF band. This brings difficulties to understand HRV results and makes LF/HF ratio an inaccurate measurement of the balance between the sympathetic and parasympathetic systems. Above problem also has been found in studies on many other areas and precludes the clinical application of HRV analysis (18, 35).

To overcome the inability of current methods of HRV analysis, we have recently developed and validated a novel mathematical technique to accurately isolate the sympathetic and parasympathetic dynamics within ANS, based on modified principal dynamic mode (PDM) analysis (62). The PDM is a nonlinear method because it models heart rate series with quadratic Volterra-Wiener kernels (36). Then eigenvalue decomposition is applied to select most significant components from a series of basis functions that construct the kernels. These components correspond to the most essential dynamics of the nonlinear system, which should correspond to the sympathetic and parasympathetic dynamics in the case of HRV analysis. Thus, it is a dimension-reduction technique based on the assumption that noise components will have smaller eigenvectors and eigenvalues than the signal components of interest, and thus, they are rejected. Using pharmacological agents that selectively block the two branches of the ANS in healthy human subjects, we have shown that the nonlinear PDM algorithm is more accurate than the PSD in describing the activities of the sympathetic and parasympathetic regulations (63).

Therefore, applying PDM in diving studies, we can obtain more accurate estimation of the ANS activity than using the traditional PSD method. Currently there are only two

studies that assess ANS responses in real SCUBA diving and no such studies on DCS. And these two studies obtained different results regarding LF and LF/HF values of HRV. Nevertheless, the PDM method is able to give a better quantification of the physiological responses to hyperbaric stress and DCS. It may also help to predict the potential risks during diving.

Specific Aims

The principal dynamic mode method will be employed to estimate the dynamics of the autonomic nervous activity during SCUBA diving and decompression sickness induced in swine. The specific aims of the proposed research are:

1) Using human subjects, estimate the modulation of the ANS in different hyperbaric environments (underwater and hyperbaric chamber), and quantify the differences in the dynamics of the autonomic nervous activity between normobaric and hyperbaric conditions.
2) Similarly, in the swine model, estimate the modulation of the ANS during decompression sickness, and compare the dynamics of the ANS pre- and post-DCS.
3) The final aim is to find a marker of the dynamics of the ANS that may be indicative of the incidence of the decompression sickness.

Hypothesis

First, we hypothesize that, during diving, the parasympathetic and cardiac sympathetic activities increase progressively with the increase of diving stress.

Second, DCS induces dramatic changes in both sympathetic and parasympathetic nervous systems, and the integrity of the ANS could be impaired due to deleterious effects of DCS. Furthermore, there is a critical point of change in the ANS dynamics during the development of DCS. Finding this critical point will be helpful in predicting the onset of DCS, thus a treatment can be applied to prevent the exacerbation of DCS.

Materials and Methods

The ANS activity is evaluated in three experiment protocol: dives in dry hyperbaric chamber, underwater SCUBA diving and inducement of DCS in swine. The first two are human studies, which help to understand the ANS activity in different hyperbaric environments. Their results also can serve as the baseline, compared to DCS condition. The model of swine DCS is induced in a hyperbaric chamber by rapid decompression, which has been applied in many DCS related studies (17, 34). Through this model, we can measure the ANS modulations during pre-dive, dive, decompression and post-dive, thus find the critical point of DCS development.

Experiment Protocols

Hyperbaric Chamber Dives Involving Human Subjects

11 volunteers of professional divers (10 male and 1 female, 27-55 years old) participated in this study at John T. Mather Memorial Hospital, Port Jefferson, NY. The divers were first compressed with oxygen, then with air on another day.

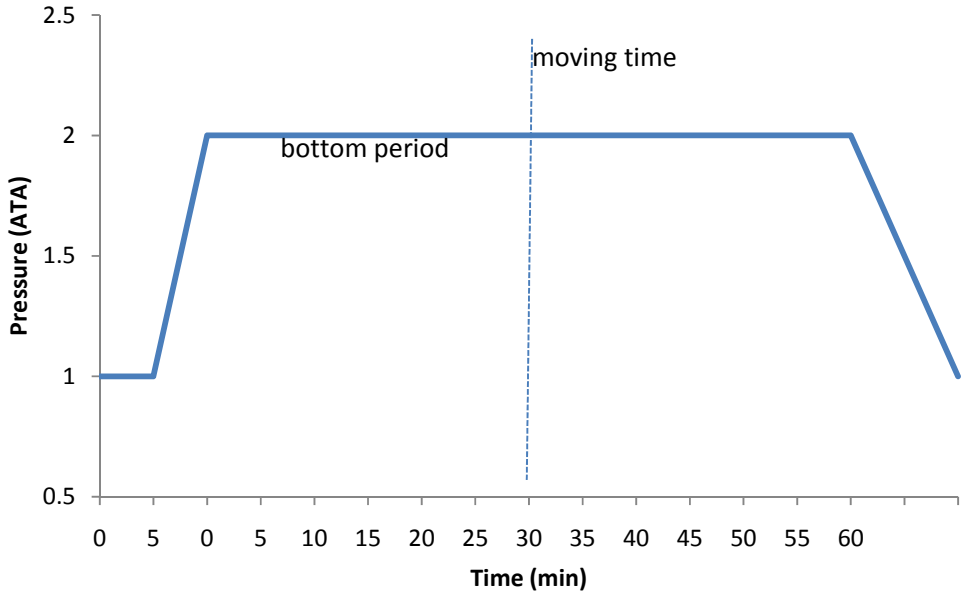

Figure 2. The protocol of hyperbaric treatment with both oxygen and air

During the oxygen dive, divers changed into approved hyperbaric attire and were instructed on restrictions involving a hyperbaric chamber. Patient history and vital signs were obtained for each diver. Then the divers were told to lie down and minimize

movement during data collection. A 12 lead ECG was monitored (Hewlett Packard Merlin Multi-Parameter Monitor) and ECG data were fed into a computer by a PowerLab data-acquisition system (PowerLab, Model ML750, ADInstruments). A baseline ECG reading was obtained for 15 minutes prior to dive. Then the diver began to descent to 2 ATA at 3 psi/min in a hyperbaric chamber (Sechrist 3200, Sechrist, CA) ventilated with 100% oxygen. If the diver had a problem with ear equalization, the descent would be slowed as needed to accommodate the diver. Divers stayed at 2 ATA for one hour with continuous recordings of ECG. They were allowed to move for 1-2 minutes after 30 minutes at 2 ATA. After 1 hour of data collection at high pressure, divers began to ascent to 1 ATA at 3 psi/min.

At least 2 days after the oxygen dive, divers returned to perform the air dive. During the air dive, divers wore a Scott Mask to breathe air (21% oxygen) from external supply. The dive profile of the air dive was the same with that of the oxygen dive (Figure 2).

The ECG signals at 2 ATA were divided into 5 minute segments. The R waves in these segments, as well as in the last 5 minutes of baseline ECG, were detected for further analysis of HRV.

SCUBA Dives of Human

Twenty four professional divers participated in this study. Divers were randomly assigned to perform dives at different depths and with different breathing gases. Each diver participated in multiple dives. SCUBA dives were carried out at 5 different depths (33, 66, 99, 150 and 200 ft) with 3 different breathing gases (air, nitrox and trimix). Table 1 summarizes in detail the dive protocols for all depths.

Table 2 Summarized information of SCUBA dives

Depth	Bottom Duration	Breathing Gas	Water Temperature(°C)	# of divers	Age	Weight (kg)
33ft	30 min	Air	14.96±0.82	15	42.53±2.17	83.50±3.16
66ft	30 min	Air	12.78±0.57	16	41.13±2.03	83.28±2.85
99ft	15 min	Air	14.74±0.69	13	42.31±2.57	85.17±3.31
99ft	15 min	Nitrox	14.49±0.77	14	41.92±2.41	84.43±3.15
150ft	15 min	Trimix	12.73±0.43	12	43.08±1.83	89.77±2.19
200ft	10 min	Trimix	9.75±0.36	10	40.60±2.40	90.54±2.21

Age and weight gave the average age and weight of divers participating in each dive. Water temperature is the average temperature at bottom recorded by diving computer. Air contains 21% oxygen and 79% nitrogen. Nitrox contains 36% oxygen and 64% nitrogen. Trimix contains 10% oxygen, 50% helium and 40% nitrogen.

Prior to each dive, divers wore a five lead digital Holter ECG monitor (RZ153+, Rozinn Electronics, Cleveland, OH). ECG electrodes were securely placed on various locations of a diver's body with adhesive tape. Each diver wore a dry diving suit which insulated the Holter monitor from sea water. A diving data logger (GEO, Oceanic, San Leandro, CA) was used to record each diver's dive profile including the dive duration, depth and water temperature.

After entering water, divers floated with minimal movements in the supine position on the water surface with face out of water for 10 minutes; ECG data recorded during this phase was treated as the baseline. Once the baseline ECG recordings have been completed, divers descended to an assigned depth; when the depth was reached, divers floated with minimal movements for the pre-determined duration. The depth and bottom duration information for each dive are specified in Table 2.

Of the 10 minute ECG recordings at the surface of water, the last ast5-min segment of data was used as the baseline value. The stable parts of ECG recording at depth, also referred as the bottom time, were divided into 5 minute segments for HRV analysis. For the33- and 66-ft dives, the bottom time was as long as half an hour. Thus, we used data from these two depths to investigate diving time effect on the ANS. To understand physiological changes at different diving depths, the 3rd 5 minute time segment of the bottom time at 33, 66 and 99 ft and the 2^{nd} 5 minute time segment at 150 and 200 ft were used to perform comparisons among different depths. We chose the 2^{nd} 5 minute time segment for the 150 and 200 ft instead of the 3^{rd} 5 minute data because it takes more time to reach the bottom in the later two deep dives than the shallow dives. Specifically, the dives involved in this comparison are 33-, 66- and 99-ft dives while breathing air, but 150- and 200-ft dives were with breathing trimix gases. Finally, we studied the effect of different breathing gases on diving by comparing dives between air and nitrox at 99 ft.

Decompression Sickness Model of Swine

All following experiments were carried out at the Naval Medical Research Center (NMRC). As part of a larger study focusing on decompression sickness, DCS was induced by 2 protocols. One was a dive at 200 ft, which resulted in neurological symptoms and spinal cord injury. And another one at 60 ft mainly focused on the cardiopulmonary DCS. The animal experiments reported here were conducted according

to the principles set forth in the *Guide for the Care and Use of Laboratory Animals* (Institute of Laboratory Animal Resources, National Research Council, National Academy Press, 1996). The Institutional Animal Care and Use Committee of Naval Medical Research Center (an Association for Assessment and Accreditation of Laboratory Animal Care fully accredited facility) reviewed and approved all aspects of this protocol. All animals were maintained under the surveillance of veterinary staff.

200 ft Protocol

In the first protocol, 13 male, Yorkshire swine **(**Biotechnical Industries, Dunsborough, PA) were housed in free running cages at an animal care facility. Animals were onsite for 5 days prior to any procedures. At the housing facility, food (2-2.5% of body weight twice daily; Lab Diet Mini-Pig Grower, Quality Lab Products, Elkridge, MA) and full access to water were provided. Animals were trained daily to walk on a treadmill over three days prior to the dive. Each session lasted between 15-20 minutes, with a successful training session being defined as the swine's ability to sustain a speed of 1.5 miles/hour at 0 degree incline for 15 minutes. Animals were trained to walk on the treadmill because one of the signs used to determine the presence of DCS is the gait disturbance.

ECG electrodes were placed on the surface of body (three differential leads). An internally crafted cotton vest was then placed over the electrodes and tied in place. Next the electrocardiogram data transmitter [Jacketed External Telemetry (JET), Data Sciences Incorporation] was connected to the ECG cables. After test of data transmission, the data transmitter was removed and the animal was recovered for 1 day.

On the day of the hyperbaric exposure, ECG telemetry system was again connected and baseline signals were acquired. Next, animals were placed in a standard dog kennel and transported to the hyperbaric laboratory. While remaining in the kennel, animals were placed within the Navy's multiple large animal chamber (MLAC). The MLAC is a steel hulled hyperbaric chamber of 450 cu ft of floodable volume and pressure tested to 1,000 fsw.

The MLAC was pressurized with air to 200 fsw at a rate of 30 feet per minute. Animals were monitored via close circuit television for any signs of distress related to middle ear barotraumas (head shaking, nystagmus). Any evidence of middle ear

barotraumas resulted in a decrease in hyperbaric pressure and descent at a slower rate. Chamber atmosphere was monitored with a Geotech Anagas Dive Air Analyzers (Geotech, Denver, CO). Air composition was maintained at 21% (± 2%) oxygen and < 0.05% CO_2 surface equivalent. Temperature (80 ± 2 ^{o}F) and humidity (50 ± 5%) were controlled via an environmental control system piped to the MLAC.

After reaching 200 fsw, animals remained at this depth for a total time (from leaving surface pressure to leaving bottom pressure) of 24 to 31 minutes [referred to as bottom time (BT)]. As the main purpose of the parent study was to develop a spinal cord injury model, bottom time was adjusted through the study (24 minutes BT n= 6; 31 minutes BT n=6). After the specified BT was reached, the chamber was decompressed at a rate of 60 fsw/minute.

After reaching normal atmospheric pressure, the MLAC door was opened and the transport kennel removed. Animals were then removed from the transport kennel placed into a Panepinto sling and receive diazepam (0.125 mg/kg IV). At this time ECG signals were collected again wirelessly via the JET system into proprietary data collection software. Additional doses of diazepam (0.125 mg/kg) were allowed every five minutes to a total dose of 2mg/kg if warranted.

Animals were observed for the first hour after reaching surface pressure. Observations included animal comfort based on respiratory distress and any vocalizations (Reyes scale) and signs of DCS. Decompression sickness was noted with the onset of cutis marmorata (skin bends), or death. In this group, all 13 animals had cutis mamorata, and 4 of the animals died. After one hour the animals were assessed for comfort and returned to their holding pen. Animals unable to be immediately returned to their holding pen remained in the Panepinto sling and observed till able to return to the holding pen.

5-minute stable ECG signals were extracted from pre-dive and post-dive ECG recording separately for HRV analysis. The ECG segment from pre-dive was selected randomly; the segment from post-dive was the first 5-minute segment after surfacing.

66-ft Saturated Dive

In the second protocol, 9 neutered male Yorkshire swine (*Sus scrofa*) were examined by a veterinarian upon receipt. Prior to any procedures, animals were acclimatized for 5 days in individual free running cages with full access to environmental enrichment, water,

and food (2% of body weight daily, Lab Diet Porcine Grower 5084, PMI Nutrition, Brentwood MO).

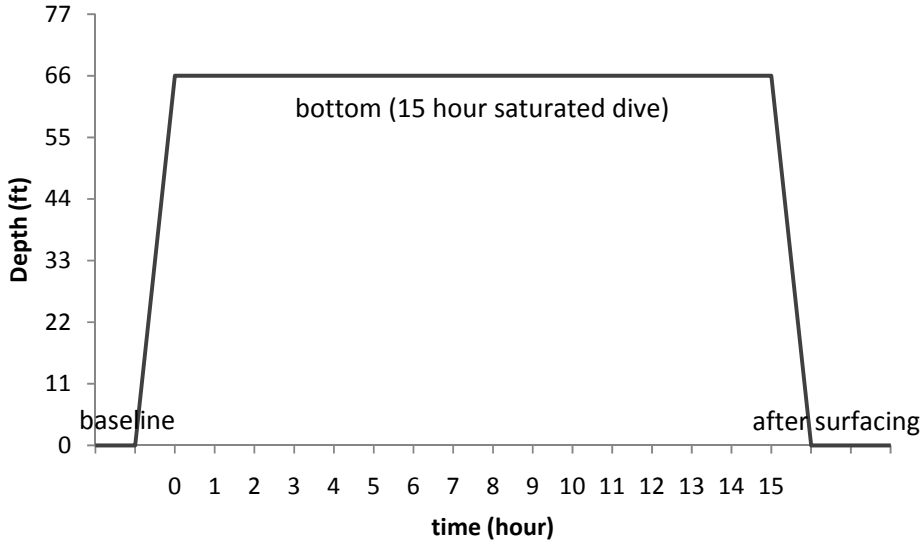

Figure 3. The protocol of hyperbaric treatment. ECG was recorded throughout the experiment. The baseline ECG before the hyperbaric treatment was around half an hour. Animals stayed at 66 fsw for 15 hours to ensure they were fully saturated. After a rapid decomposition, they were observed continuously for the first 2 hours after reaching surface pressure, and ECG was recorded at the same time.

On the day prior to hyperbaric exposure, animals underwent Electrode placement on the body surface (three differential leads) and sterile external jugular vein catheter placement. Anesthesia induction was performed with intramuscular injection of 20 mg/kg ketamine and 2 mg/kg xylazine (Ketaject 100 mg/ml, Xyla-Ject 100 mg/ml, respectively; Phoenix Pharmaceutical, St. Joseph, MO). Anesthesia was maintained with 2-5% isoflurane (Halocarbon Products, Rover Edge, NJ) via a face mask. The external jugular vein was catheterized with a 16 gauge by 20.3 cm single lumen catheter (Braun Certofix; B. Braun Medical Inc, Bethlehem, PA) via the modified Seldinger technique (9) and advanced until 8-10 cm extended from the skin incision site. The catheter was sutured in place with an exit site on the dorsal thorax, taped to the skin, and then brought through a vest worn by the animal which also was placed over the electrodes and tied in place. Vests accommodated a 76 cm long, 8 cm diameter Tygon™ tube sheath (Cole-Parmer, Vernon Hills, IL) through which the catheter was advanced on the day of the dive. Electrocardiogram data transmitter [Data Sciences Incorporated's jacketed external telemetry (JET)] was connected to the electrocardiogram (ECG) cables, and after

verification of transmission the unit was removed, and the animal recovered for 1 day. Limited ambulation was assessed in the box during the observation period; full ambulation after recovery was verified prior to return to the holding pen, where the animal remained overnight.

On the day of the hyperbaric exposure, the subjects were placed into individual custom designed Plexiglas™ boxes (26"x54"x38") inside a steel hulled 450 $ft.^3$ hyperbaric chamber as reported elsewhere (33). Each box allowed for an adjustable atmosphere environment in which the subjects could breathe without requiring restraints. Subjects had access to water *ad libitum* via a lixor fitted to the boxes. The external jugular vein catheter was connected to a sterile line, fed through a Tygon™ tube secured to the torso vest and a 360° swivel on the ceiling of the Plexiglas box, which allowed the animal to move freely and to make postural adjustments without twisting the line. The ECG telemetry system was re-connected, and baseline signals were acquired.

The chamber was pressurized with air to 184 kPa (60fsw) at a rate of 92 $kPa \bullet min^{-1}$ (30 fsw/min) and remained at depth for 15 h. Subjects were monitored via close circuit television for any signs of distress related to middle ear barotrauma. Chamber and box atmospheres were monitored with separate gas analyzers (Geotech Anagas Dive Analyzer, Denver, CO). The chamber O_2 concentration was maintained at 21% (± 2%) and CO_2 at < 0.05% surface equivalent. Temperature was maintained between 23.9-29.4ºC (75-85^oF) with 50% (± 5%) humidity via an environmental control. After 15 h animals underwent decompression at 92 $kPa \bullet min^{-1}$ (30fsw/min).

Baseline ECG signals were recorded starting 30 min before the hyperbaric exposure, continued throughout the saturation period, and for 120 min after surfacing or until death/euthanasia. Note that the baseline data were not available from 2 swine as the ECG signals were highly corrupted with noise so that accurate RR intervals could not derived. All parameters related to the PSD and PDM were calculated for each 5 min segment, then averaged over 30 min. "Bottom" refers to the first half hour after animals reached 184KPa (60 fsw); "surface" is the period after decompression but before DCS onset. It should be noted that DCS onset varied from as short as 10 min to as long as 1 h. If the surface period was > 30 min, only the first half hour of the data were used. We used data segments for analysis following diagnosis of cutis marmorata (cutis) and

cardiopulmonary (CP) DCS as determined by a trained observer. In certain cases, both cutis and CP symptoms occurred simultaneously.

Data Analysis Method

All data analysis method introduced here were completed in Matlab 7.0 (Mathworks, MA).To perform HRV analysis, HR data must first be extracted from 5-minute segment of ECG data. In the hyperbaric study, the sampling rate of ECG was 400 Hz; in SCUBA diving, it was set to 180 Hz; in the swine study the sampling rate of 750 Hz was used. The sampling rate was determined by different devices used in different experiments. For example, for SCUBA diving, we used a Holter monitor which had a pre-set sampling rate of 180 Hz. For ECG data from SCUBA diving, heart rate is extracted by the software (Holter for Windows+, Rozinn, Cleveland, OH) of the Holter monitor. In the other two studies, heart rate is detected by recognizing R wave in ECG with a derivative/threshold algorithm which we have developed. Particularly in the swine experiments, after QRS complex detection, a search window using a threshold proportional to T decay rate determined the position of the T wave terminus (29). Then ECG morphology parameters, such as the QRS duration, ST amplitude, T wave amplitude, QT interval and QT interval corrected for heart rate (QTc) were calculated and averaged for every 5 min of data.

Time and Frequency Domain Analysis

Our data analysis consisted of both time and frequency domain methods. Time domain parameters of HRV include the standard deviation of R-R intervals from successive 5-minute periods (SDNN), the root-mean square of the successive difference of R-R intervals (RMSSD) and approximate entropy (ApEn) (2). SDNN measures the overall level of ANS activity. RMSSD is a measurement of localized variance within R-R intervals, thus reflects high frequency variation in HR and is associated with parasympathetic activity. ApEn quantifies the complexity of a given system. It is calculated based on the recommended embedding dimension and the threshold value of m=2 and r=0.15, respectively (43). It is utilized in HRV analysis with the assumption that abnormalities of ANS are related to the reduced complexity of ANS.

Before calculating HRV parameters in frequency domain, HR data are first resampled to 4 Hz, and then interpolated to 1 Hz for human data and to 2 Hz for swine

data. PSD of HR series are calculated with the method of the Welch periodogram. A 128-point FFT is applied, using Hanning window and 50% overlapping segments. For human, LF band is widely defined as 0.04-0.15 Hz, and HF band is 0.15-0.4 Hz. For swine, the LF and HF bands are denotes as 0.04-0.2 and 0.2-0.6 Hz respectively, which are in agreement with previous studies and the observation of the PSD of our swine data (26, 51). As mentioned in Introduction section, HF represents the parasympathetic modulation, and LF is controlled by both sympathetic and parasympathetic systems.

Analysis of HRV using PDM

The PDM method, originally introduced by Marmarelis, is a method based on extracting only the principal dynamic components of the signal via eigen decomposition (36). The PDMs are calculated using Volterra-Wiener kernels based on expansion of Laguerre polynomials. The application of PDM in HRV analysis was introduced in our previous publication (63). Its main idea is described in detail in the following paragraphs.

The general input-output relation of a stable nonlinear time-invariant system can be given by the Volterra series as following:

$$y(n) = k_0 + \sum_{m=0}^{M-1} k_1(m)x(n-m) + \sum_{m_1=0}^{M-1}\sum_{m_2=0}^{M-1} k_2(m_1,m_2)x(n-m_1)x(n-m_2) + \ldots$$

where $x(n)$ is the input and $y(n)$ is the output of the system. M is the memory of the system, which is set as 60 in this study. k_i denotes the Volterra kernels, and the quadratic kernel k_2 describes the nonlinearity of the system. The estimated output with a maximum lag M can be expressed in a matrix form:

$$\hat{y}(n) = \mathrm{X}^T(n)Q\mathrm{X}(n)$$

where T denotes transform, the vector $\mathrm{X}^T(n)$= [1 $x(n)$ $x(n\text{-}1)$ … $x(n\text{-}M\text{+}1)$] is composed of the input M-point epoch at each time n and a constant 1 that allows incorporation of the lower-order kernel contributions, and Q is a $(M+1)\times(M+1)$ matrix of Volterra kernels with

$$Q = \begin{bmatrix} k_0 & \frac{1}{2}k_1(0) & \frac{1}{2}k_1(1) & & \frac{1}{2}k_1(M-1) \\ \frac{1}{2}k_1(0) & k_2(0,0) & k_2(1,0) & \cdots & k_2(0,M-1) \\ \frac{1}{2}k_1(1) & k_2(0,1) & k_2(1,1) & & k_2(1,M-1) \\ & \vdots & & \ddots & \vdots \\ \frac{1}{2}k_1(M-1) & k_2(M-1,0) & k_2(M-1,1) & \cdots & k_2(M-1,M-1) \end{bmatrix}$$

Then these kernels can be expanded based on L Laguerre functions:

$$y(n) = c_0 + \sum_{j=0}^{L-1} c_1(j) v_j(n) + \sum_{j_1=0}^{L-1}\sum_{j_2=0}^{L-1} c_2(j_1, j_2) v_{j_1}(n) v_{j_2}(n) + \ldots$$

where

$$v(n) = \sum_{m=0}^{M-1} b_j(m) x(n-m)$$

and $[b_j(m)]$ are the Laguerre functions calculated with Laguerre coefficients α=0.5. The number of Laguerre functnions L is 6 or 8 usually. Then Q can be constructed with the estimated kernels (c_0, c_1, c_2) in following way:

$$Q = \begin{bmatrix} c_0 & \frac{1}{2}c_1^T B^T \\ \frac{1}{2}Bc_1 & B^T c_2 B \end{bmatrix}$$

where $B = [b_0^T \quad b_1^T \quad \ldots \quad b_{L-1}^T]$. Laguerre functions are chosen as an appropriate orthonormal basis because they exhibit exponential decaying properties that make them suitable for physiological systems modeling. In addition, due to basis function expansion, the estimation accuracy is maintained even with a small data length.

Since c_2 is a real symmetric square matrix, it can always be decomposed: $c_2 = R^T \Lambda R$, where the eigenvector matrix R will always be an orthonormal matrix, and Λ is the diagonal eigenvalue matrix. The second order kernels are solved by $B^T R^T$, and Λ reveals the relative importance of each kernel. We select only the significant kernels based on eigenvalues, as the principal dynamic modes of the system.

The above algorithm theoretically requires white noise as the input to a system. Because only single HR data are available and the real input to a physiological system cannot be as irregular as white noise, a broadband input signal is constructed from the

original heart rate series. We first use a time-varying autoregressive model to track the original HR data, and then the residual between the estimated signal and original signal is taken as the input of the PDM method. The parameters of the model are estimated by the method of time-varying optimal parameter search (TVOPS) developed by our lab (14), which ensures the performance of tracking. Other tracking techniques also can be used, such as least mean square and time-invariant autoregressive model.

Once the PDMs of HR are obtained from the constructed input, since ANS plays a main role in HR regulation, the two most dominant PDMs in HR usually characterize the dynamics of the parasympathetic and sympathetic nervous regulations respectively. Other eigenvectors are rejected since they may be related to noise or nonessential dynamics. More important, dynamics of sympathetic and parasympathetic systems are separately represented by two dominant PDMs, thus the problem of PSD method is avoided. These two PDMs were converted into frequency domain by FFT to quantify the strength of PDMs by power spectrum. The PDM representing the sympathetic system still has its dominant peak in the LF band of HRV, so we named it as LF PDM. The PDM of the parasympathetic system contains frequency components from both LF and HF ranges, because the parasympathetic activity within LF range is also captured by this PDM. With its majority power still in HF range, this PDM is named as HF PDM. Hereafter, we also have a LF/HF ratio of PDM to reveal the balance between two nervous systems.

In summary, PDM method quantifies the nonlinearity within ANS activity and separate dynamics of sympathetic and parasympathetic systems accurately. Thus, the derived PDMs' two main dynamics, LF and HF PDM are also referred to here as the sympathetic and parasympathetic dynamics respectively.

Statistics

In both human studies, experiments data are divided into 5-minute segments. For example, in human chamber study, there are one 5-minute segment of baseline and 10 segments of diving, and we need to investigate the difference among many different time segments. Thus, the one-way analysis of variance (ANOVA) with repeated measurement is applied in human hyperbaric experiment. When significant F ratios were obtained, Student-Newman-Keuls (SNK) tests were used for multiple comparisons.

In SUBA diving experiment, data are represented as mean ± standard error. During the investigation on the time effect of diving, the one-way repeated measurement analysis of variance (ANOVA) was performed to compare parameters at different time segments. In each dive, parameter values at the second or third 5-minute time segment were regarded as the bottom value and compared to the baseline by the paired t-test. To compare among different depths, the difference between the baseline and bottom was first taken for the dives at each depth, and then ANOVA was employed to compare these diving-induced alterations at different depths. When significant F-ratios were obtained by ANOVA, Student-Newman-Keuls (SNK) tests were used for multiple comparisons. For the comparison of air and nitrox gas dives, the difference between the baseline and bottom was also taken, and a t-test was used instead of ANOVA. A p value < 0.05 was considered significant.

In swine studies, data are represented as mean ± standard deviation. The paired t-test was employed in the first swine protocol when comparing the baseline with post-DCS condition. The null hypothesis was rejected when p-value < 0.05. In the 66-ft dive protocol, the one-way (ANOVA) was performed to measure the difference among groups. When significant F ratios were obtained, Fisher's Least Significant Difference (LSD) tests were used for multiple comparisons. A p-value < 0.05 was considered significant.

All statistics were performed in SigmaStat 3.0 (SPSS Inc., Chicago, IL).

Results

Hyperbaric Chamber Dives Involving Human Subjects

During hyperbaric treatment, subjects were allowed to move a little to release the discomfort that resulted from keeping still for a long time. The time segment containing the moving time was not analyzed, which is from the 30^{th} to 35^{th} minute of each dive. Additionally, the last time segment usually contained artifacts or was not as long as 5 minutes, so it was also not analyzed. In both air and oxygen dives, majority of HRV parameters showed a trend of increase, but the alterations during oxygen exposure were more significant.

The results in hyperbaric and hyperoxic condition are shown in Table 3. Heart rate decreased progressively, as the time at pressure elapsed. This decrease in the heart rate became statistically significant, after diving for 35 minutes. HF PDM and RMSSD increased during the treatment. They both became significantly different with baseline when time in the chamber lasted for more than 15 minutes. SDNN also significantly increased after 20-minute dive. However, this increase was not significant during the time segments from the 40^{th} to 50^{th} minute. LF and HF of PSD did not alter significantly, though they showed a trend of slight increase. LF PDM was also unchanged throughout the treatment.

In air dives, there were no significant changes for all parameters except HF PDM (Table 4). But it only exhibited the significant increase between the 35^{th} and 40^{th} minute of hyperbaric treatment. Although HR, SDNN and RMSSD showed a similar trend of increase as in the oxygen dive, these changes were not significant.

Table 3 HRV parameters of baseline, and hyperbaric (2 ATA) and hyperoxia (100% oxygen) treatment

	Baseline	Dive5	Dive10	Dive15	Dive20	Dive25	Dive35	Dive40	Dive45	Dive50	Dive55
HR	65.74±8.30	61.94±9.30	60.41±8.48	59.41±8.18	59.87±8.06	59.77±7.60	59.4±7.41	58.62±6.59*	57.64±6.96*	57.46±70*	57.99±6.52*
LF_PDM	0.098±0.041	0.089±0.022	0.103±0.023	0.095±0.021	0.121±0.037	0.106±0.019	0.116±0.034	0.106±0.021	0.095±0.024	0.094±0.03	0.098±0.014
HF_PDM	0.153±0.038	0.165±0.046	0.181±0.042	0.16±0.039	0.201±0.037*	0.187±0.048*	0.181±0.033*	0.194±0.032*	0.185±0.026*	0.183±0.041*	0.186±0.032*
RMSSD	33.33±17.22	44.18±23.66	46.75±21.99	48.88±21.51*	48.51±21.49*	49.55±18.71*	49.43±20.76*	50.91±20.71*	51.29±21.44*	54.44±23.46*	54.74±22.14*
SDNN	47.12±17.39	60.52±15.09	57.59±13.95	59.75±17.47	65.07±16.87*	65.62±15.59*	63.3±16.91*	62.1±15.49*	57.56±9.02	60.55±12.63	66.14±14.26*
LF_PSD	4.63±3.05	6.66±6.07	5.42±5.57	5.78±7.21	5.64±5.68	4.67±4.72	4.41±3.09	4.99±4.19	3.67±3.03	3.62±3.71	4.72±3.38
HF_PSD	2.19±1.17	2.91±2.84	3.45±2.94	3.2±2.53	3.29±2.42	3.16±1.84	3.22±2.03	3.13±1.83	2.74±1.73	3.17±2.01	3.37±2.16

Dive5 represents the first 5-minute segment of hyperbaric treatment, and dive10 represents the segment from 5^{th} to 10^{th} minute, and so on.
*P<0.05 when compared with baseline value

Table 4 HRV parameters of baseline and hyperbaric treatment (2 ATA) when breathing air

	Baseline	Dive5	Dive10	Dive15	Dive20	Dive25	Dive35	Dive40	Dive45	Dive50	Dvie55
HR	66.02±10.40	64.13±7.70	63.35±7.13	63.63±6.78	63.07±7.33	62.5±7.10	62.02±7.74	61.43±7.40	61.29±8.03	62.51±6.01	61.91±6.44
LF_PDM	0.113±0.034	0.114±0.027	0.113±0.034	0.105±0.036	0.105±0.023	0.127±0.029	0.114±0.050	0.12±0.024	0.111±0.04	0.138±0.027	0.106±0.045
HF_PDM	0.156±0.029	0.190±0.039	0.180±0.051	0.178±0.044	0.192±0.055	0.184±0.038	0.227±0.064*	0.199±0.04	0.188±0.054	0.209±0.033	0.176±0.030
RMSSD	34.08±18.63	40.92±14.76	39.94±15.47	39.22±14.16	46.31±24.26	44.15±19.63	46.61±21.77	49.17±26.68	46.14±26.51	40.59±13.89	37.81±12.67
SDNN	54.39±29.34	65.23±17.51	64.33±29.37	64.32±19.66	72.77±27.65	80.91±37.98	76.03±27.67	77.99±32.03	70.82±34.22	75.61±23.68	61.02±14.04
LF_PSD	6.29±5.06	8.44±5.30	6.50±4.94	6.48±5.19	7.18±3.85	7.66±5.48	8.32±5.49	7.35±4.29	7.30±5.25	7.12±3.74	5.57±3.02
HF_PSD	2.12±0.79	2.76±2.04	3.46±3.56	3.14±2.38	3.57±2.99	2.69±1.47	3.26±2.46	3.93±3.42	3.06±2.10	2.88±2.37	2.24±1.63

*P<0.05 when compared with baseline value

Table 5 HRV parameters during the 33ft dive

	Baseline	Dive5	Dive10	Dive15	Dive20	Dive25	Dive30
HR	99.51±2.04	94.25±3.80*	89.16±2.99*	85.98±2.69*	84.29±2.31*	83.66±2.27*	84.17±1.99*
Sympathetic	0.145±0.009	0.149±0.008	0.133±0.011	0.148±0.016	0.158±0.010	0.144±0.009	0.148±0.010
Parasympathetic	0.178±0.008	0.233±0.022*	0.212±0.020*	0.225±0.028*	0.234±0.023*	0.245±0.018*	0.238±0.019*
RMSSD	14.70±1.88	19.61±7.36	20.01±2.07	23.25±2.80*	25.64±3.21*	29.73±4.01*	26.59±2.82*
SDNN	33.75±4.41	43.02±2.22	40.71±3.64	41.80±3.48	46.24±3.88	48.76±3.53*	52.69±3.84*
LF	12.82±2.74	16.92±3.22	15.14±3.04	13.42±2.29	14.93±3.16	14.03±2.44	17.11±3.42
HF	2.75±0.49	4.24±1.13	2.72±3.79	3.60±1.22	3.20±0.86	5.48±1.56	4.59±1.30

Dive5 represents first 5-minute segment of dive, and dive10 represents from 5^{th} to 10^{th} minute, and so on.
*P<0.05 when compare with baseline

Table 6 HRV parameters during the 66ft dive

	Baseline	Dive5	Dive10	Dive15	Dive20	Dive25	Dive30
HR	101.41±2.93	95.11±3.87	87.05±3.57*	84.2±3.12*	81.72±2.61*	80.29±2.48*	81.92±2.34*
Sympathetic	0.130±0.009	0.162±0.013	0.163±0.016	0.156±0.017	0.152±0.015	0.164±0.024	0.175±0.011
Parasympathetic	0.194±0.020	0.258±0.030*	0.221±0.019	0.268±0.034*	0.279±0.032*	0.285±0.023*	0.257±0.023*
RMSSD	13.44±1.94	29.21±6.99*	30.86±7.72*	38.47±8.41*	43.76±8.78*	47.36±8.99*	44.12±7.80*
SDNN	36.74±5.19	55.80±8.90*	53.14±9.35*	54.79±9.03*	64.10±9.79*	67.94±10.27*	73.17±9.93*
LF	11.32±3.43	23.74±3.29	27.46±10.98	19.98±7.74	24.24±8.65	25.37±6.94	26.72±7.81
HF	2.00±0.44	6.96±0.88	7.18±2.51	7.33±2.53	8.83±3.03*	9.87±2.72*	11.02±3.09*

*P<0.05 when compare with baseline

Time Effect of Diving

Figure 4 shows two typical diving profiles of the 33-ft and 66-ft. As shown in the figure, these divers were able to maintain the desired depth for the entire duration. However, only 11 of 16 divers were able to maintain the instructed depth and data recordings for 30 minutes. Thus, only 11 subjects' data were used to study the time effect of diving.

For the 33-ft dive, HR during the bottom period was significantly lower than the baseline, as shown in Table 5. The parasympathetic dynamics significantly increased throughout the bottom periods when compared to the baseline. The increase of RMSSD was significant after diving for 10 minutes. There was also an increase of SDNN at 33 ft for duration of 20 minutes. However, other parameters, the sympathetic dynamics, LF and HF of PSD did not show any significant alterations during the dive, although there was a trend of increase in the LF and HF values of the PSD.

The results of the 66-ft dive are summarized in Table 6. The HR of the baseline was higher than that of the bottom period. The parasympathetic dynamics increased significantly throughout the dive. Both RMSSD and SDNN values increased significantly when compared to the baseline. The HF significantly increased compared to the baseline when time at the bottom lasted for more than 15 minutes. In the 66-ft dive, there was only a slight increase of the LF and the sympathetic dynamics during the bottom stage.

In both dives (33 ft and 66 ft), the parasympathetic parameters, including the HF, RMSSD and the parasympathetic dynamics, all continued to increase from the beginning of dives, until they reached a peak value between the 20^{th} and 25^{th} minute of dives, and then decreased at the last segment of dive data. However, the HR decreased as the dive continued and reached the lowest point at the 5^{th} five minute segment, and then increased at the 6^{th} time segment of the bottom time. Meanwhile, the sympathetic dynamics and the LF of PSD did not show clear trend throughout these two dives.

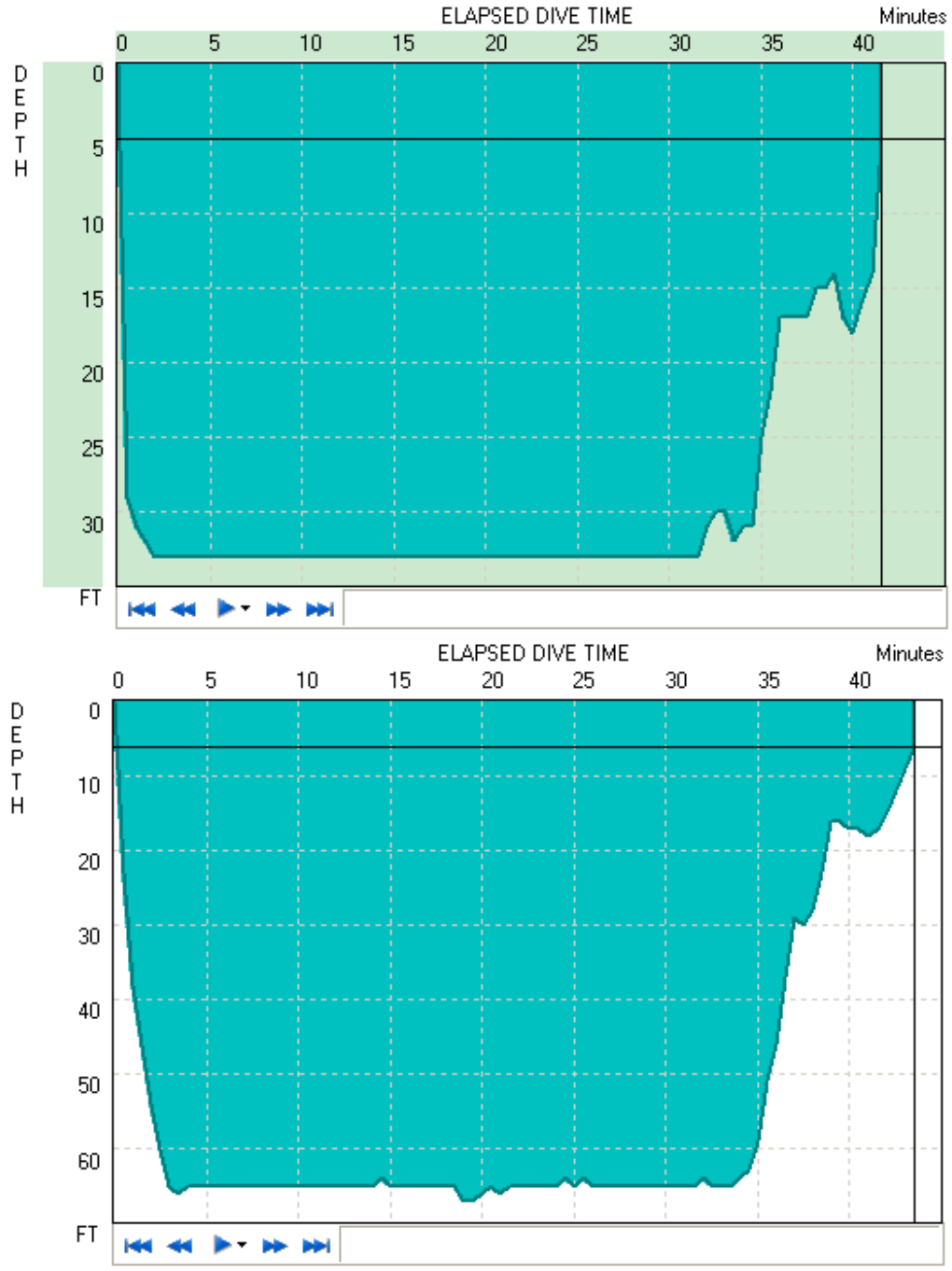

Figure 4. Typical dive profiles of the 33-ft (top) and 66-ft (bottom) dives, respectively.

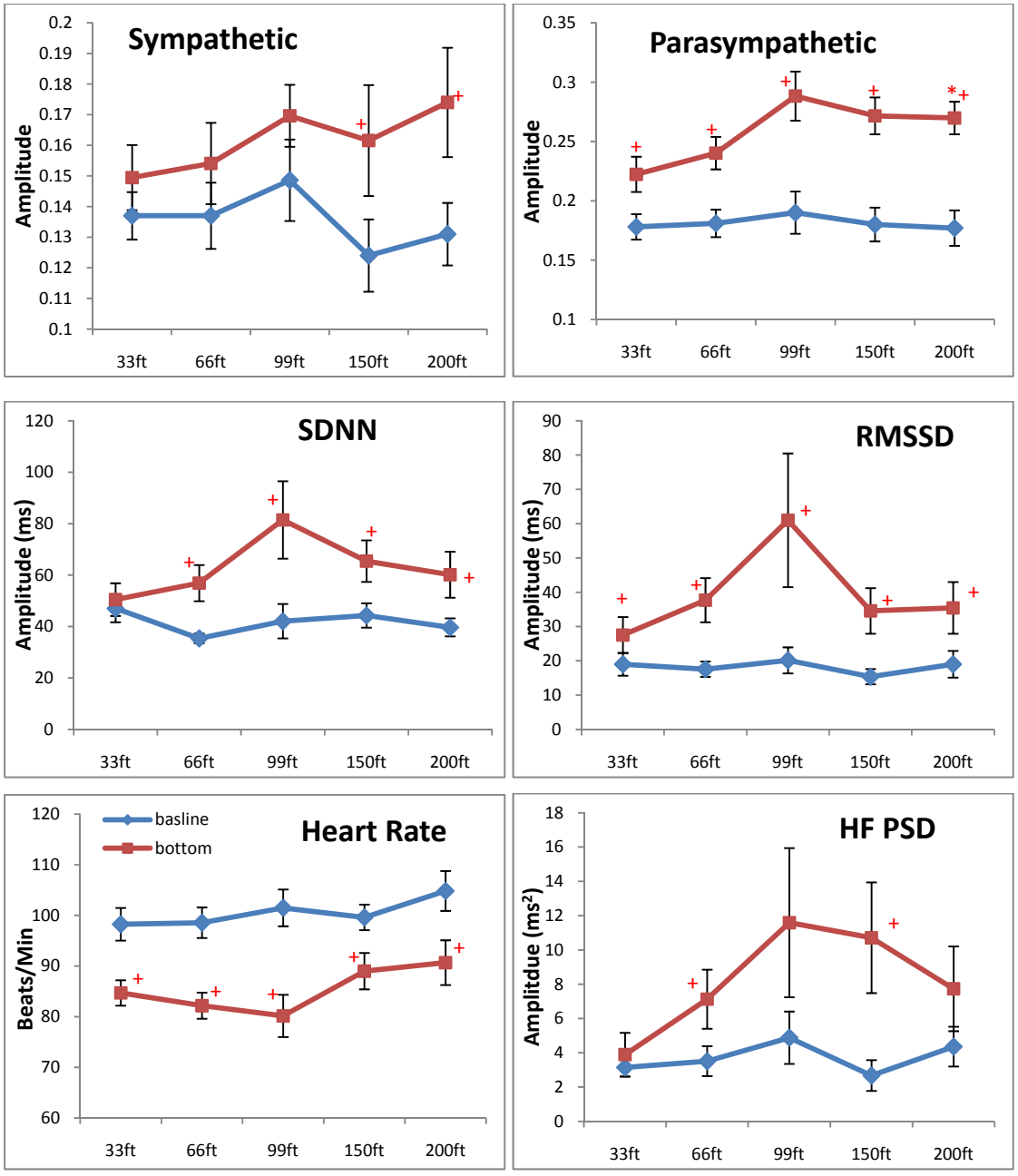

Figure 5. Depth comparison of HRV parameters. The red line marked with diamond represents baseline, the blue square line is bottom condition. + means $p < 0.05$ when comparing the bottom to its corresponding baseline by paired t-test. * means $p < 0.05$ when comparing to the 33-ft condition.

Depth Comparison

For all dives at different depths, the heart rate at the bottom showed a significant decrease when compared to the baseline (Figure 5). Both RMSSD and the parasympathetic dynamics increased significantly at the bottom. The HF also increased at

all depths when compared to the baseline, but this increase was significant only at 66 and 150 ft. Both the LF and the sympathetic dynamics at the bottom increased when compared to the baseline. Additionally, the increase of the sympathetic dynamics was significant at 150 and 200 ft. The SDNN, reflecting overall ANS tone, also showed significant increase during diving at 66, 99, 150 and 200 ft.

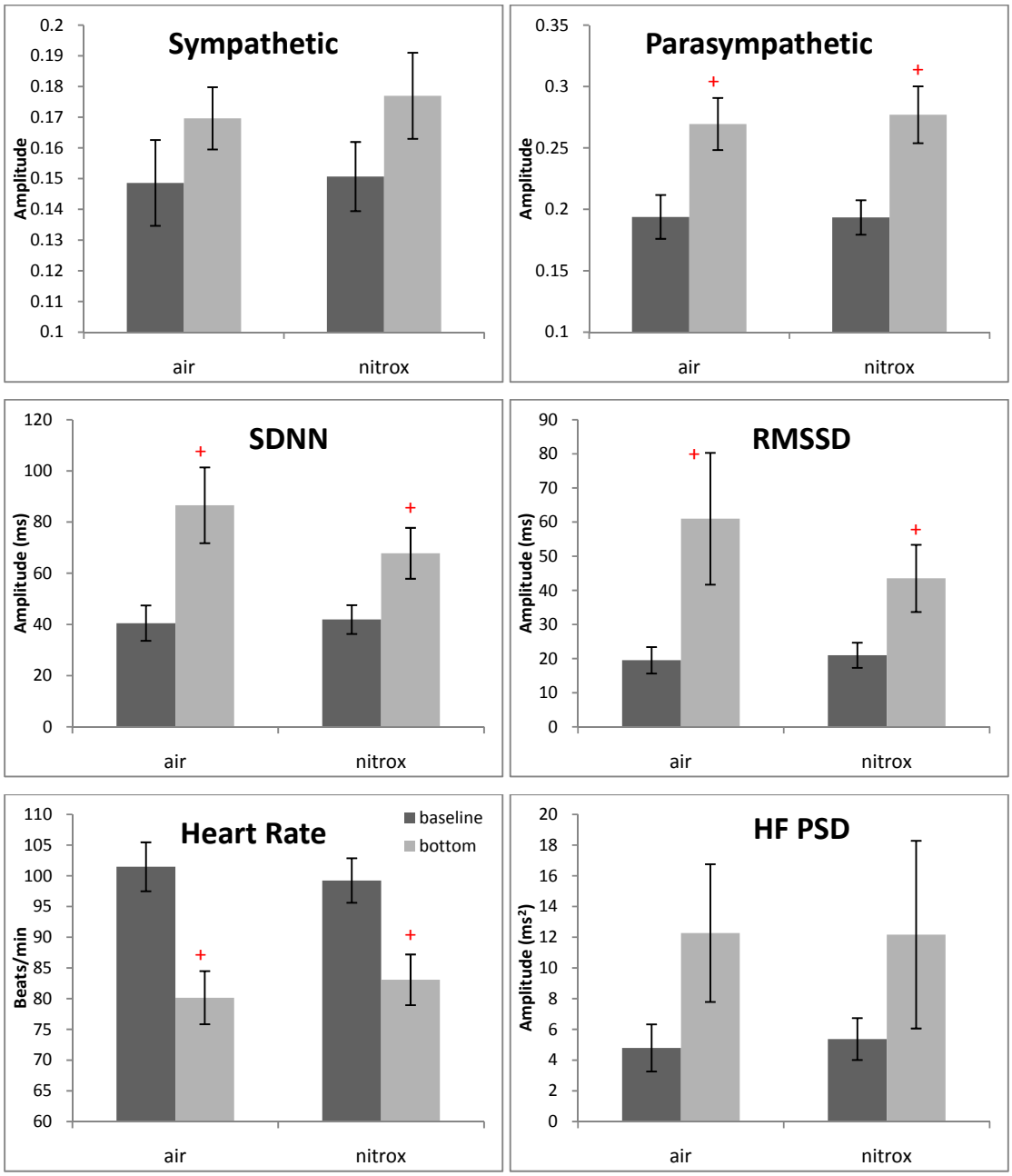

Figure 6. Effects of breathing gases on HRV parameters. The black bar represents baseline and the grey bar represent bottom condition. + means $p < 0.05$ when comparing the bottom to its corresponding baseline.

When comparing among different depths, diving induced increase of the parasympathetic dynamics at 200-ft dive was significantly higher than the 33-ft dive. However, other parameters did not show a significant difference at different depths. It can be note that, the bottom values of the RMSSD, HF and the parasympathetic dynamics reached their maximum at 99-ft dive (Figure 5). As the diving depth increased, the sympathetic dynamics showed a trend of concomitant increase.

Effect of Breathing Gases

For the 99-ft dives, both air and nitrox gases were used. These two dives induced a decrease in the HR and an increase in the SDNN, RMSSD and the parasympathetic dynamics, which is similar to other dive depths. However, as shown in Figure 6, no significant differences were found in these parameters between the air and nitrox gas dives. The bottom values of these parameters were nearly at the same level for the two gases.

Decompression Sickness Model of Swine

Neurological DCS

The quantification of HR variability (the inverse of the R-R intervals) was performed in both time and frequency domains. The time-domain parameters (mean HR, variance of HR, RMSSD of R-R, and ApEn) all showed a decreasing trend with DCS. However, none of these parameters is significantly different between the baseline and DCS conditions.

Table 7 Comparison of time-domain parameters between baseline and DCS conditions. None of the parameters show significant difference between the two conditions.

	Heart Rate (beats/min)	Variance of HR	RMSSD	ApEn
Baseline	123.63±18.72	6.90±1.72	21.38±17.83	1.17±0.09
Post DCS	109.14±39.49	5.13±1.96	21.87±17.80	1.00±0.24

Representative parasympathetic and sympathetic dynamics via the PDM at baseline and post-DCS are shown in Figure 7. The group average showing the significant decrease in the magnitude of these tracings with DCS is provided in top and bottom panels of Figure 8 for the PSD and PDM methods, respectively. Both methods show a significant decrease in the average spectral power, post-DCS compared to baseline. The spectral power in both LF and HF, and sympathetic and parasympathetic dynamics obtained by the PDM, all show significant decreases with post-DCS. The observed decrease is on the order of 55% for the sympathetic and 58% for the parasympathetic dynamics post-DCS, using the PDM method. The decrease in the LF and HF powers post-DCS are greater than the PDM with reductions of 65 and 69%, respectively. Variability in the results is less with the PDM, since its level of significance is higher (sympathetic, $P = 0.001$ vs. $P = 0.003$; parasympathetic, $P = 0.002$ vs. $P = 0.04$) than the PSD.

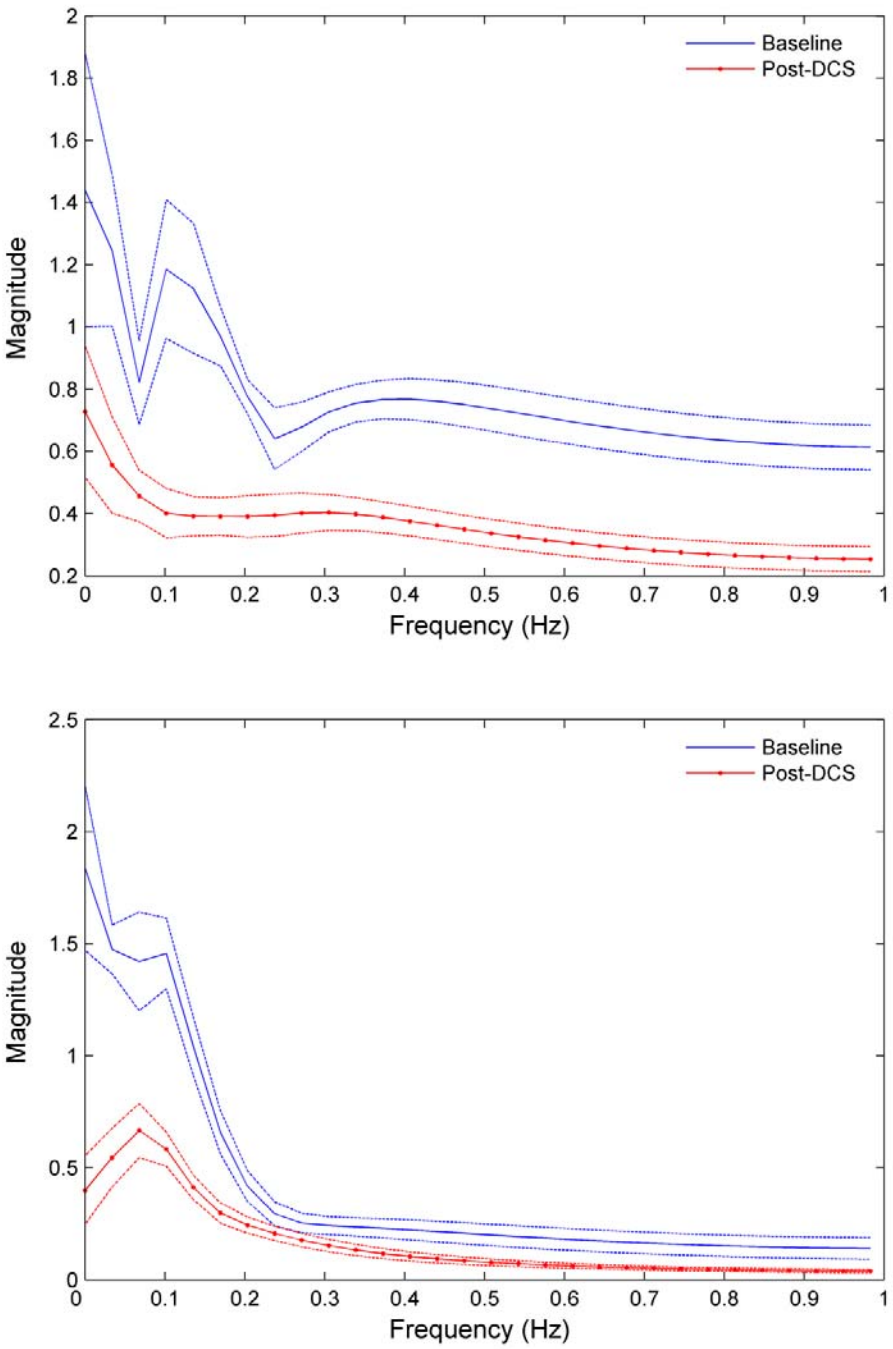

Figure 7. Averaged principal dynamic modes pertaining to the parasympathetic (top panel) and sympathetic (bottom panel) tones during baseline (blue) and post-DCS (red) conditions. Solid and dotted lines represent averages and their standard errors.

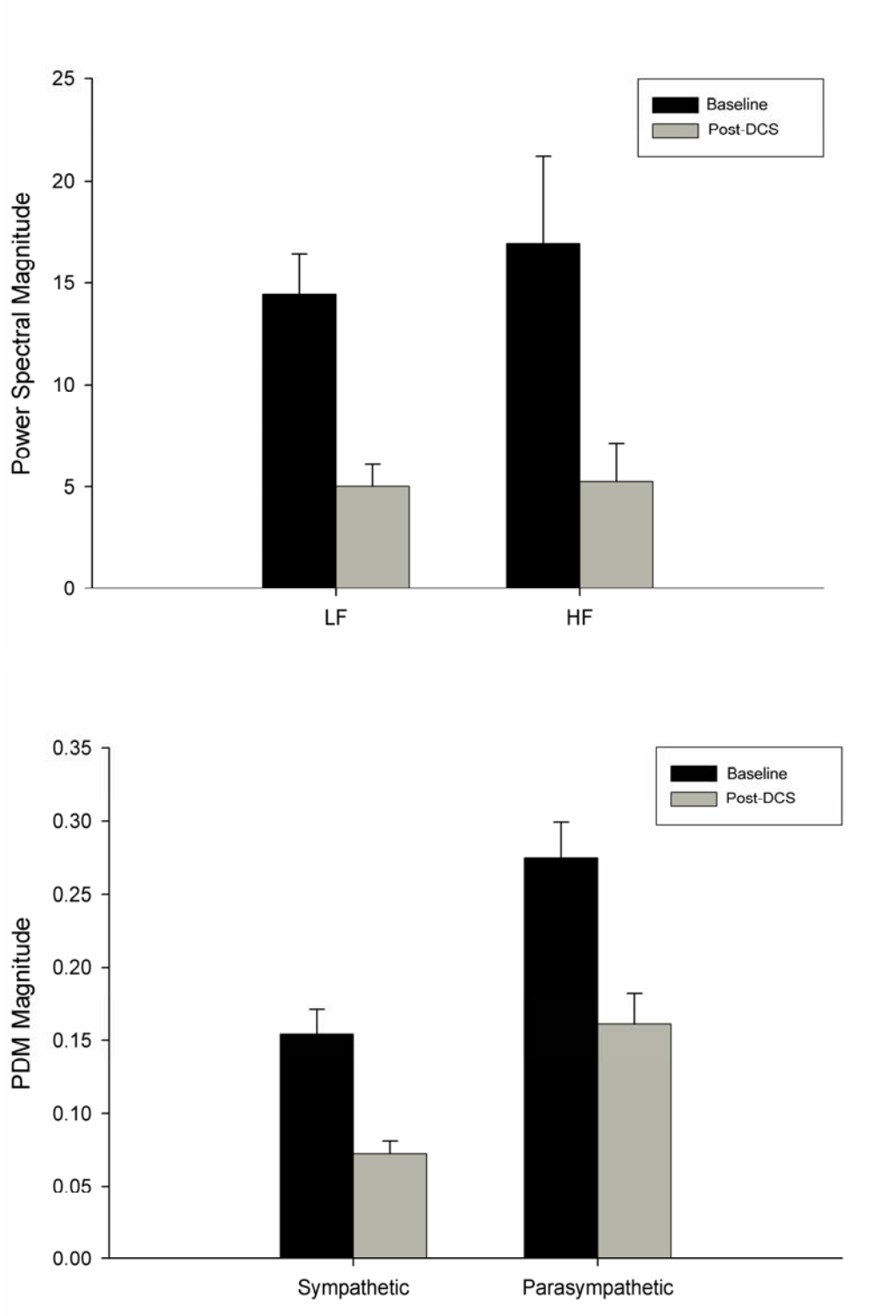

Figure 8. Comparison of baseline and post-DCS for PSD (top panel) and PDM (bottom panel) methods. Both methods show significant decrease ($P < 0.05$) in magnitudes of LF and HF via PSD, and sympathetic and parasympathetic via PDM during DCS when compared to the control condition.

Cardiopulmonary DCS

The 9 swine (72.06 ± 4.16 kg) all manifested cutis DCS. Six (66%) had concomitant cardiopulmonary (CP) signs, indicating both Type I and Type II DCS. No neurological signs were manifested.

Table 8 The time of events that occurred after surfacing

Event	Minutes after surfacing
Cutis	37.78±23.83
CP (n=6)	41.67±27.01
RMSSD	10.00±15.00*†
HF	12.22±15.63*†
Parasympathetic	9.44±6.35*†

For cutis and CP, the table shows the average onset time of these two symptoms. For RMSSD, HF and the parasympathetic dynamics, the table lists the average time when the post-dive values of these parameters first became higher than their mean values at bottom. 6 subjects developed CP, so n=6 for it. For other events, n is equal to 9.
* $p<0.05$ when compared to cutis
† $p<0.05$ when compared to CP

Table 8 shows the average time of onset of cutis and CP DCS after surfacing. CP DCS onset ranged widely from 14-88 min; CP DCS occurred simultaneously with, or after onset of, cutis DCS.

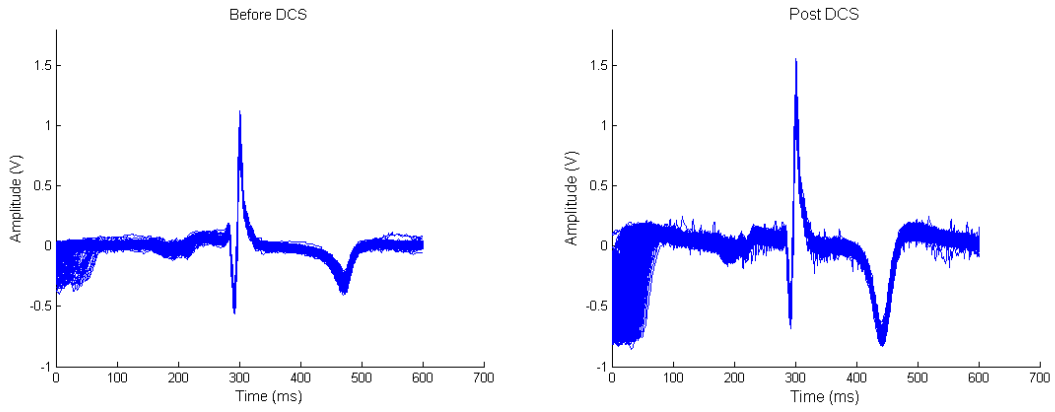

Figure 9. The overlapped ECG of 300 beats at surface (left panel) and post-DCS (right panel)

ECG Morphology

One ECG cycle of 300 overlapped and aligned beats from a representative subject is shown in Figure 9. The left panel shows the aligned and overlapped ECG tracings of 300 beats collected immediately after the animal reached the surface and before DCS onset. The right panel shows the ECG following onset of cutis DCS. T-wave amplitude increased and the QT interval decreased after DCS onset. The group average (Table 9)

indicates that this increase of T-wave amplitude is statistically significant. Additionally, the QT interval after surfacing significantly exceeded that of baseline. The QRS duration, ST amplitude and QTc did not differ among groups, however (Table 9).

Table 9. Heart rate and ECG morphologies at different phases of the experiment

	Heart Rate (beats/min)	QRS duration (s)	ST elevation (V)	T wave Amplitude (V)	QT interval (s)	QT c
#Baseline(n=7)	127.33±11.24	0.0638±0.0013	0.00625±0.0070	-0.293±0.091	0.239±0.013	0.346±0.017
Bottom (n=9)	110.34±10.12*	0.0635±0.0016	0.0132±0.0068	-0.275±0.150	0.264±0.023	0.356±0.020
Surface (n=9)	95.29±14.62*	0.0640±0.0017	0.00856±0.0078	-0.245±0.114	0.273±0.021*	0.342±0.020
Cutis (n=9)	109.55±21.35*	0.0640±0.0018	0.00215±0.0152	-0.458±0.193†	0.254±0.024	0.338±0.026
CP (n=6)	120.07±20.37†	0.0640±0.0020	0.00952±0.0367	-0.477±0.259	0.247±0.028	0.343±0.030

* $p < 0.05$ compared to baseline
† $p < 0.05$ compared to surface
# n = 7 because the baseline data were significantly contaminated with noise for 2 swine.

Hyperbaric Effect

Following the hyperbaric exposure, the PDM's sympathetic dynamics underwent a statistically significant decrease, whereas the parasympathetic dynamics underwent a statistically significant increase compared to the baseline (Figure 10). Similarly, the LF decreased and HF increased, but these changes were not significant; the HR was significantly reduced, however.

After Decompression

The HR nadir occurred after surfacing and prior to DCS onset (Figure 10). The parameters SDNN, RMSSD, HF and the parasympathetic dynamics significantly increased compared to baseline. The SDNN and RMSSD parameters were also significantly higher than their bottom stage values.

In Table 8, three parameters representing the parasympathetic tones are shown: RMSSD, HF power and the parasympathetic tone via PDM. These three parameters can predict the onset of DCS based on the observation that the parasympathetic tones significantly increase compared to baseline and bottom stages in swine experiencing CP or cutis DCS (see also Figure 10). We note parasympathetic tone obtained via the PDM approach has the fastest prediction of DCS onset and cutis followed by RMSSD and then HF. By using increased parasympathetic power, we can predict the onset of either cutis or CP DCS far earlier than their actual occurrence as noted by an expert observer.

After decompression, the sympathetic dynamics elevated (P<0.05) compared to their bottom values, and reached a level similar to baseline (Figure 10). LF power followed a similar but non-significant trend.

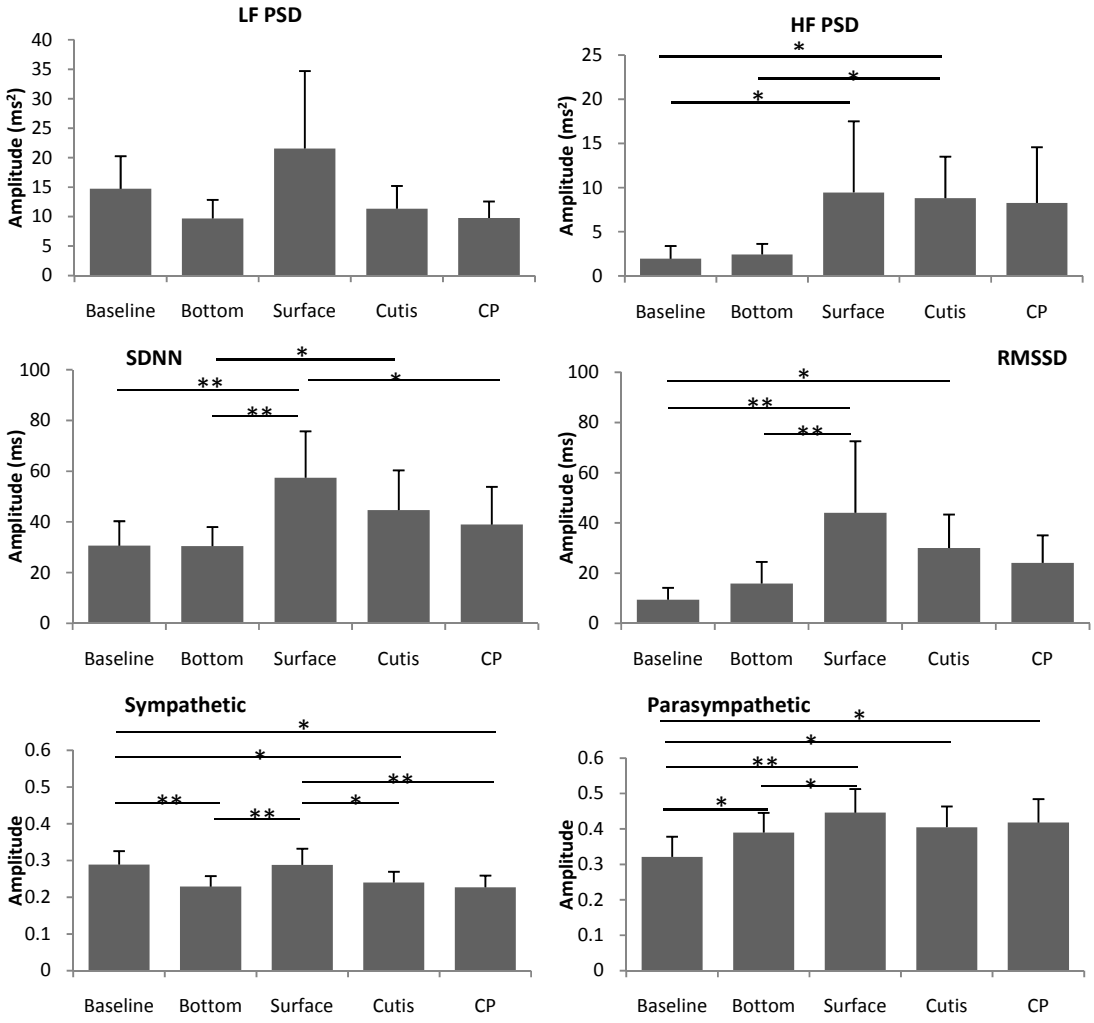

Figure 10. Changes in HRV parameters throughout the experiment. Except LF of PSD, all other parameters exhibited significant difference among different conditions. * means p<0.05 when comparing two groups. ** means p<0.01 when comparing two groups.

Post DCS

Following cutis or with CP DCS onset, HF and the parasympathetic dynamics were elevated compared to both baseline and bottom stages, but a significant decrease in SDNN occurred compared with the period right after surfacing (Figure 10); there was a concomitant non-significant trend of decrease in RMSSD. After onset of cutis DCS, RMSSD, HF and the parasympathetic dynamics were significantly higher than baseline,

and HF also significantly exceeded its value at the bottom stage. Following CP DCS onset, the parasympathetic dynamics were still significantly higher than baseline, and the SDNN decreased to a level less than its value upon surfacing. The LF and the sympathetic dynamics decreased gradually from time of surface to cutis and CP DCS onset, but only the latter was significant. Further, with cutis and CP DCS, the sympathetic dynamics were significantly lower when compared to baseline and pre-DCS condition after decompression. As shown in Table 9, the HR gradually increased and approached its baseline value during the time from surfacing to cutis and CP DCS onset.

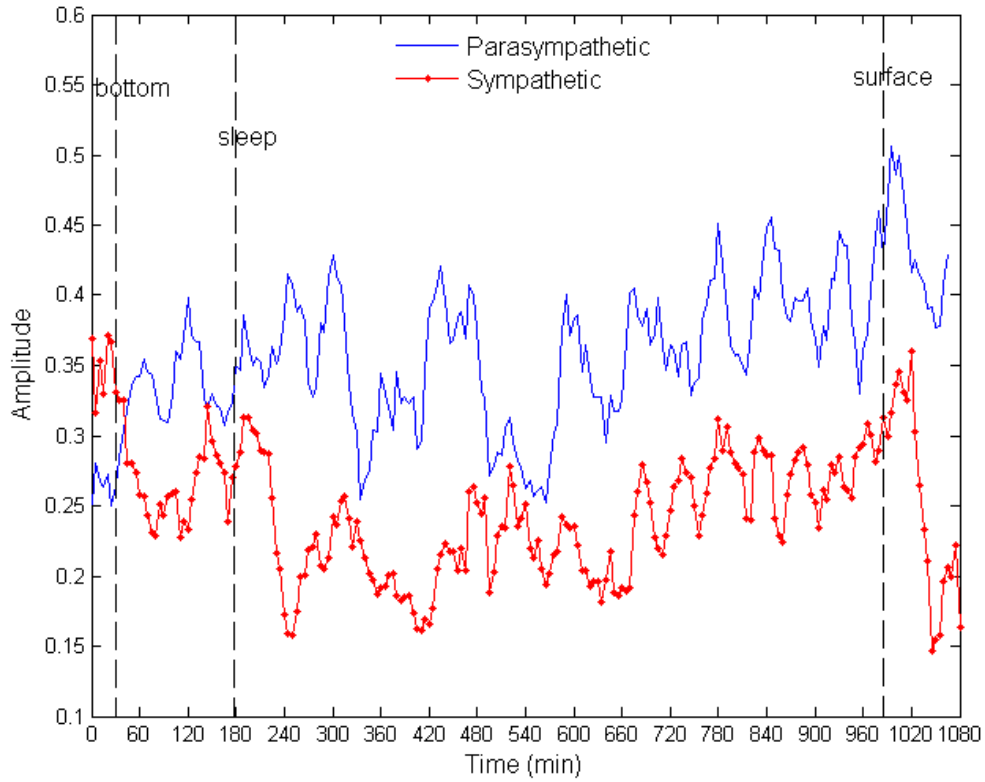

Figure 11. The sympathetic and parasympathetic dynamics throughout the entire experiment from a representative subject. The sympathetic (dotted) and parasympathetic (solid) dynamics were obtained through PDM method. The vertical dash lines indicate the beginning time of different stages of the experiment.

Fig. 11 shows the sympathetic and parasympathetic dynamics of a representative subject throughout the entire hyperbaric exposure and post-surfacing observation period. It tracks the changes of the ANS dynamics during different stages of the exposure as

described above. Note that during sleep stage, the parasympathetic modulation was at a higher level than the baseline, bottom stage, and sympathetic tone.

The changes in the sympathetic and parasympathetic dynamics for each experimental stage for all swine subjects are shown in Figure 12. As shown, most swine showed consistent trends as they undergo transition from the baseline to the cutis stages. In particular, all 9 swine exhibited increased ANS dynamics as they transitioned from the bottom to surface stage.

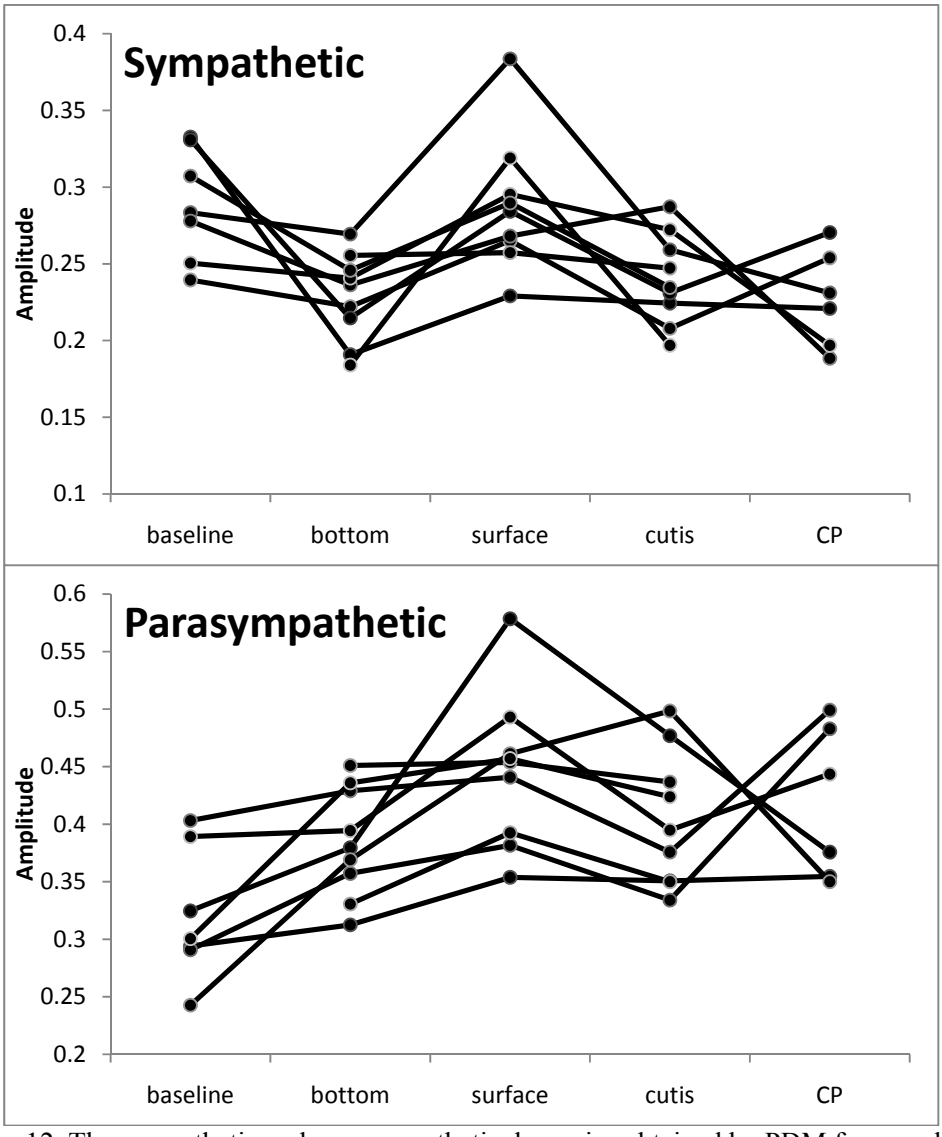

Figure 12. The sympathetic and parasympathetic dynamics obtained by PDM from each subject at different experiments phases. Please note that 2 subjects did not have baseline and 3 subjects did not developed CP DCS.

Discussion

Hyperbaric Chamber Dives Involving Human Subjects

In this experiment, we found that, at 2 ATA bradycardia is primarily induced by hyperoxia but not by hyperbaria. At this pressure, the increased activity of the parasympathetic nervous system is indicated by RMSSD and HF PDM, but no signs of the sympathetic alteration were found.

When breathing air in the hyperbaric chamber, there were nearly no significant alterations in the parameters that we measured. There was no obvious bradycardia (66.02±10.40 vs. 61.29±8.03, baseline vs. lowest HR during hyperbaric treatment, $P>0.05$). The slight increases of RMSSD, HF of PSD and HF PDM indicate the increase in the parasympathetic activity which should be the cause of bradycardia. The unchanged LF PDM suggests the absence of sympathetic alteration. However, evidences of increased parasympathetic activity and decreased sympathetic activity were observed in previous studies (31, 59). The main reason is that we used a pressure of 2 ATA, which is lower than the pressure in the previous studies (2.5 or 3 ATA). The pressure of 2 ATA may have failed to produce enough hyperbaric stress on professional divers.

In hyperbaric (2 ATA) and hyperoxic (100% oxygen) condition, significant alterations were induced in several parameters. The HR became significantly reduced when time in the chamber lasted for more than 35 minutes. An increase of the parasympathetic activity was indicated by the significant increase of RMSSD and HF PDM, which is the cause of HR reduction. However, we did not find the signs of the sympathetic alterations in our parameters, since LF PDM and LF PSD did not change significantly. Therefore, the significant increase of SDNN should be attributed to the increase of the parasympathetic activity. These results regarding the ANS activity are similar to those obtained by HRV analysis in a pure oxygen environment at the pressure of 2.5 ATA (31). Compared to the results of the air dive, it is the hyperoxia that plays the central role of inducing these significant changes.

It has been shown that hyperbaria (3 ATA) and hyperoxia (100% oxygen) is able to separately induce the decrease of the sympathetic activity and the increase of parasympathetic activity (31, 49, 59). The decreased sympathetic activity induced by hyperbaria or hyperoxia was only indicated by the measurement of MSNA, but not by the

LF of PSD, in previous studies. It is either because the effects of hyperbaria or hyperoxia on cardiac sympathetic activity are different with their effects on peripheral sympathetic activity, or because HRV analysis as a non-invasive method is not as sensitive as MSNA measurement in detection of the sympathetic alterations. In the environment of hyperbaric hyperoxia, previous studies only applied the PSD method of HRV analysis to evaluate the ANS activity. The results in these studies, as well as in our study, confirmed an increase of the parasympathetic activity, but failed to find the alteration of the sympathetic tone. This implies that, the combined effects of hyperbaria and hyperoxia on the sympathetic system may be different with their individual effects. Future studies employing the measurement of MSNA or catecholaminergic transmitter may be helpful to clarify the ANS activity in a hyperbaric hyperoxic environment.

The mechanisms of hyperbaria- and hyperoxia- induced bradycardia have been suggested by researchers. Hyperbaria balances the hydrostatic pressure within the systemic circulation, and shifts the blood from the vein to the central circulation. The increased venous blood return may stimulate the arterial baroreceptor or cardiopulmonary receptors, thus reduce the heart rate. But the mechanisms of hyperoxia-induced bradycardia are unclear. It could be related to arteriolar induced vasoconstriction by breathing oxygen. The function of vasoconstriction is to reduce the blood perfusion to organs and maintain a constant level of oxygen supply. Arteriolar vasoconstriction increases blood pressure and results in bradycardia via a vagally mediated baroreceptor reflex (50). Another factor is the suppression of arterial or carotid chemoreceptor afferent discharge (48). It lowers the HR by eliminating tachycardiac effects of the sympathetic branch of the ANS.

The long-term studies at relative high pressure (>24 ATA) show that changes in HR and HRV occur in the initial stage of hyperbaric exposure, and they return to normal values thereafter. In the air dive, a similar trend can be seen in RMSS, SDNN, LF PSD, HF PSD and HF PDM. They started to increase at the beginning of bottom time and reached a peak value between the 30^{th} to 40^{th} minute of air dives. However, this trend is not so obvious in the oxygen dive. Some parameters increased until the end of dives.

PDM parameters performed better than PSD parameters since LF and HF of PSD did not show any significant difference in either air or oxygen dive. RMSSD is also quite sensitive to the parasympathetic changes in this study.

SCUBA Dives of Human

In all dives, a decrease in the HR and a dominance of the parasympathetic regulation were observed despite different diving depths and breathing gases when compared to the baseline. For 33- and 66-ft dives, the parasympathetic dynamics increased as the diving duration increased. As the diving depth increased, divers should be experiencing more diving stress. However, breathing gases did not show different effects on the ANS activity even at the greater depth level. To our knowledge, this is the first study that evaluates the effects of time duration, different depths and breathing gases in SCUBA dives. For two other published SCUBA dives with the aim of examining the ANS during diving, one was carried out in a swimming pool (46) and the other involved recreational dives all at shallow depths (15).

The baseline values were collected when the divers floated on the water surface without face immersion. A heavy gas tank and a dry suit added extra load burden to divers and resulted in a much higher HR (around 100 bpm at surface) than without them. However, the workload burden is the same at the baseline and bottom since divers donned the same gas tank and dry suit for both stages of diving.

Our dive experiments were performed in a relative low water temperature (17.8 °C at the surface). A previous study has shown that a body immersion in water of 14 °C induces an increase of heart rate and metabolic activity (54). The bottom water temperature in this study was around 14 °C (Table 2), but in our study, we have observed decreased HR at the bottom stage. This difference could be attributed to donning a dry suit which prohibited a heat loss and the several degrees reduction in temperature from the water surface to the bottom was not a main factor influencing the ANS activity in this study. Thus, the physiological changes between the baseline and diving are mainly induced by a diving reflex, increased ambient pressure, high density of breathing gas and psychological stress.

Time Effect

For the 33- and 66-ft dives, the decreased HR and increased parasympathetic parameters (HF, RMSSD and the parasympathetic dynamics) during diving illustrate the dominance of the parasympathetic system (Table 5 and 6). During the entire bottom duration, the above noted parasympathetic parameters showed an increasing trend until the 25th minute of the bottom time and then decreased at the last 5-min segment of dives. We believe this decrease in the last segment is due to the fact that some divers did not stay at the bottom but began ascending to the surface. In summary, we found that the ANS dynamics gradually change to adapt to underwater environment but our time duration of 30 minutes was not enough to reach a steady state during SCUBA diving. This time effect certainly should be considered in any diving studies. Thus, in the depth comparison of this study, we used the 3rd 5 minute time segment of the bottom time at 33, 66 and 99 ft and the 2nd 5 minute time segment at 150 and 200 ft to perform the comparison among varying depths, because it takes approximately 5 more minutes to reach the bottom stage with deeper dives.

In these two depths (33 ft and 66 ft), the sympathetic dynamics and LF of PSD during diving were not significantly different when compared to the baseline and did not show a clear trend throughout the bottom time. This suggests that the sympathetic regulation was not changed in these shallow dives and the alterations of SDNN were mainly induced by the parasympathetic system.

Depth Comparison

At all depths, the HR at the bottom decreased compare to the baseline. Moreover, RMSSD and the parasympathetic dynamics show a significant increase. In the 200-ft dive, the difference of the parasympathetic dynamics between the baseline and bottom was significantly higher than the 33-ft dive (Figure 5). This suggests an enhanced parasympathetic modulation in deep dives compared to the 33-ft dive. The values of the parasympathetic parameters reached a peak at 99-ft, and then slightly decreased for the 150- and 200-ft dives. At different depths, the sympathetic dynamics increased compared to the baseline. But this increase was significant only for the 150- and 200-ft dives, indicating a greater sympathetic modulation in these two dives compared to shallower dives.

After face immersion, diving reflex and water pressure induce the bradycardia and the activation of the parasympathetic system to redistribute body blood and conserve heat for vital organs (19, 38). As the depth increases, increased water pressure may further contribute the process of blood redistribution and increase the parasympathetic modulation. In our study, this phenomenon was observed as the parasympathetic modulation increased with increasing depth up to 99 ft. However, for the150- and 200-ft dives, an increase in the sympathetic modulation and a decrease in the parasympathetic regulation were observed when compared to the 99-ft dive. The most possible cause of this result is the psychological stress that individual encounters in underwater. Previous studies have shown that that mental stress causes the sympathovagal balance to be tilted towards the sympathetic system (41, 52). More importantly, mental stress can also attenuate the amplitude of diving reflex (45). However, we believe the parasympathetic modulation was still dominant in the 150- and 200-ft dives because bradycardia was present in these two dives. Thus, the sympathetic activation and the parasympathetic decrease, compared to 99-ft dive, were not significant.

Effects of Breathing Gas

As the ambient pressure increases during diving, the density and partial pressure of gas components in breathing gas mixture also increase. Among different gas components, a high density of oxygen can induce bradycardia, decrease of the sympathetic activity and an increase of the parasympathetic modulation. The mechanism of hyperoxic bradycardia is under debate and remains unresolved. The possible reason could be that the hyperoxia induces arteriolar vasoconstriction, or reduces input stimuli to the peripheral or central chemoreceptors (48, 50). Thus, in this study, the increased partial pressure of oxygen may have contributed to the diving-induced bradycardia and the increase of the parasympathetic modulation.

In order to quantify the contribution of the oxygen pressure, we have assessed the ANS modulation while breathing air and nitrox during 99-ft dives. However, no difference was found in the HR and the ANS modulation between air and nitrox dives. In a normobaric condition, significant differences in the HR and the parasympathetic modulation were observed when the proportion of oxygen in breathing gas was as high as 70% (49). This may suggests that more than 3-fold difference in oxygen concentration is

needed to induce significant physiological changes. Since nitrox contains 36% oxygen, which is not too much higher than that in air, thus not high enough to induce physiological difference between two dives. Another possibility is that because the diving reflex and water pressure have already increased the parasympathetic modulation to a very high level, hyperoxia condition cannot further enhance the parasympathetic activity. Thus, changes in the oxygen concentration are unable to induce significant ANS alterations. In summary, we speculate that different breathing gas mixtures do not significantly change the ANS dynamics because the oxygen concentrations were not all different in varying gas mixtures. Thus, the main factors inducing the ANS changes among varying depths are mainly different pressures and mental stress, and not different gas mixtures.

In conclusion, this experiment found predominance of the parasympathetic system in SCUBA diving, which is consistent with previous diving studies (15, 46), as well as hyperbaric chamber studies (31, 32). We have also found that it take considerable time for the ANS to reach a steady state in the underwater environment. As the diving depth increases, mental stress may become an important factor influencing the ANS activities. Nitrox and air do not have different effects on the ANS in the 99-ft dive. Monitoring the ANS status through PDM method provides a good assessment of physiological changes during diving and it can be used as a potential tool for predicting and avoiding hazardous diving conditions.

Decompression Sickness Model of Swine

Neurological DCS

The primary finding of this experiment is the significant reduction in both the sympathetic and parasympathetic tones post-DCS when compared to pre-dive baseline. Parameters derived from both PSD and PDM method are reduced and reveal more than a 55% reduction in the two branches of the ANS, when the swine exhibited symptoms of DCS.

The evidence of the spinal cord injury was verified in the deceased animals by H&E staining (Figure 13). The spinal cord injury was diffuse in nature and consisted of hemorrhage and axonal degeneration. In addition, based on random sampling of the four

of the surviving animals, we found all had pathological evidence of spinal cord injury. Our results are in agreement with a previous study which also found spinal cord injury with DCS (11). In addition, the clinical observation of Cutis Marmarota which is often used as one of the acknowledged signs of DCS was observed in all swine. The Cutis Marmarota is often associated to consist of vascular congestion, vasculitis as well as neutrophilic infiltration and reactive changes in endothelial cells. These changes are most evident in the capillaries and venules. In other studies the time of onset of cutis marmarota has correlated with severity of DCS (10).

Figure 13. The injured spinal cord from a swine with DCS

We defined the LF of both PSD and PDM in the range of 0.04-0.2 Hz and the HF of 0.2-0.6 Hz. These LF and HF ranges concur with previously-defined frequency ranges for the swine model, and are also consistent with the frequency peaks found in our spectrum. These LF and HF ranges extend beyond those found in humans (LF: 0.04-0.15 Hz; HF: 0.15-0.4 Hz), presumably because swine have higher heart rates and higher spectral power (>0.4 Hz). The PDM, unlike the PSD, is able to separate the two branches of the ANS, thus, we were able to show dynamics pertaining to the parasympathetic and the sympathetic nervous system (Figure 7). Note that the parasympathetic dynamics via the

PDM show significant magnitudes in both low (0.04-0.2 Hz) and high (0.2-0.6 Hz) frequencies, whereas the sympathetic dynamics from the PDM only show significant power in the LF (0.04-0.2 Hz) range. Clearly, this is the advantage of the PDM over the PSD method, since the dynamics of parasympathetic system resident in LF range can be accurately attributed to HF PDM. This advantage has also been demonstrated in human subjects in our previous two studies.

The significant reduction of LF and HF PDM, as well as LF and HF of PSD, suggests the severe depression of both branches of ANS. However, the mechanisms of DCS-induced impairment of ANS are not clear yet. The spinal cord injury described above is most likely the culprit of this impairment in our study, as the symptoms of spinal cord injury appeared in all subjects. Bubbles in spinal cord can cause venous block and hemorrhage (as shown in Figure 13), and spinal cord ischemia. They can also damage tissues within spinal cord directly, especially myelin sheath, because of its high solubility for N_2. Thus, the efferent nerves of ANS within spinal cord also can be damaged, when spinal cord injury of DCS occurs. Subsequently the ANS loses its regulation to control the heart rate, and consequently the HRV parameters are dramatically decreased.

Cardiopulmonary DCS

In this experiment, we identified elevated parasympathetic system activity before and during the DCS development, as well as reduced sympathetic modulation post-DCS when compared to the baseline and at surfacing. This is in stark contrast to our previous finding of a significant reduction (~50%) in both sympathetic and parasympathetic nervous activities following neurological DCS (8). In this experiment, persistent elevation of the parasympathetic dynamics during non-neurological DCS as compared to the baseline stage is most likely the compensatory effect against inert gas bubble diffusion and protection from the deleterious effects of DCS. In addition, when animals reached the surface, their HR dropped compared to both baseline and bottom stages, but there was a trend of progressive increase in HR between reaching surface and cutis/CP DCS onset.

ECG Morphology

The presence of DCS signs correlated with significantly increased T wave amplitude, compared to the pre-DCS period after decompression. A large T wave amplitude may reflect hyperkalemia (23) which probably results from DCS related acidosis (6, 13). The

post-surface QT interval prolongation indicates bradycardia during this period since this difference resolved with QT interval correction.

Hyperbaric Effects

Significant bradycardia was observed as the chamber pressure reached the 184 KPa (60 fsw) or the bottom stage. The mechanisms of hyperbaria-induced bradycardia are well documented (19). Hyperbaria alters the hydrostatic pressure within the systemic circulation, shunting blood from peripheral to central circulation. Increased venous return may stimulate the arterial baro or cardiopulmonary receptors, which then alter the efferent impulses of two autonomic nervous branches, reducing HR. We observed this phenomenon. After chamber pressurization, the decrease of the sympathetic dynamics both via the PDM and PSD, and the increased RMSSD, HF and parasympathetic dynamics all indicate increased parasympathetic activity, consequently resulting in bradycardia.

In previous chamber studies performed at similar pressures, increased parasympathetic regulation by HF has also been noted (31, 32). However, the decreased sympathetic activity was measured via muscle sympathetic nerve activity (MSNA) (59), and not the LF. Similarly in this study, the LF did not result in a statistically significant decrease; however, the parasympathetic dynamics did. This illustrates the greater sensitivity of the PDM as compared to the PSD method. By design, the PSD, as a linear method, is unable to quantify the non-linear properties of the ANS. More importantly, it cannot separate the sympathetic and parasympathetic components, especially in the LF band since it contains both dynamics.

Post-dive Elevation of the Parasympathetic Regulation

Post-decompression, the increase of RMSSD, HF and the parasympathetic dynamics when compared to the baseline and bottom stages indicates elevated parasympathetic modulation. After DCS onset, HF and the parasympathetic dynamics did not change, while RMSSD showed a slight decrease. CP DCS did not significantly depress the parasympathetic tone, but rather enhanced it. It should be noted that in our first experiment, the neurological DCS had significantly depressed both branches of the ANS dynamics (8). The decrease in LF and the sympathetic dynamics indicates a gradual reduction of the sympathetic regulation as the DCS development occurs. SDNN describes

overall ANS activity of both sympathetic and parasympathetic branches. Right after surfacing, this parameter reached its peak value and thereafter decreased, mainly due to the reduction of the sympathetic regulation.

In a chamber study from the literature involving non-DCS decompression, the HF power for the post-dive period was found to be higher than the baseline, but much lower than the bottom stage (31). This suggests that in the absence of DCS, post-dive parasympathetic tone returns to normobaric environment levels, but is still depressed compared to hyperbaric conditions. Thus, it is reasonable to speculate that the post-dive elevation of the parasympathetic modulation in this study resulted from CP DCS. In our study, the swine were fully saturated with inert gas at hyperbaric pressure of 184 KPa (60 fsw) for 15 h. Following rapid decompression, inert gas bubbles usually appear in veins and are diffused in the lung circulation where they compromise the normal exchange of oxygen, causing hypoxia and increasing plasma CO_2 (13). This is followed by chemoreflex activation, enhancing amplitude and frequency modulation of respiration (55), and aiding in the diffusion of inert gases. Since the parasympathetic activity is modulated by respiration, this increase in respiratory activity could result in parasympathetic tones enhancement. Meanwhile, the chemoreflex also increases the sympathetic activity. Bubbles also cause distention of the veins, heart and pulmonary vessels (6, 13), and consequently stretch the cardiopulmonary receptors as if there were extra blood volume in the circulation. Consequently, this decreases the sympathetic tone and increases the parasympathetic activity (44). As bubbles accumulate, pulmonary hypertension and systemic hypotension occur (6), and these subsequently increase the sympathetic tone (37). Additionally, the increase in systemic arterial pressure reduces the parasympathetic activity through the baroreflex. For the sympathetic system, the initial post-dive increase of the sympathetic modulation compared to the bottom is most likely explained by its return to a normobaric state.

After DCS onset, we observed a decrease in the sympathetic parameters of HRV compared to the surface stage. However, it seems that most of the factors discussed above should result in an increase of the sympathetic tone in DCS. Increased sympathetic activity reflects elevated HR following DCS. With pulmonary artery hypertension, a recent study found an increased muscle sympathetic nerve activity (MSNA) burst

frequency, and yet a reduced LF spectral component of HRV (37). This study suggested that the discordance between MSNA and the HRV LF parameter is due to the decline of the sympathetic neural modulation to HR. Furthermore, this is similar to the events in heart failure and may lead to sudden death in some patients with pulmonary hypertension. Considering this evidence, we speculate that in DCS there is likely an increase in the absolute amplitude of the sympathetic activity that functions to accelerate the blood circulation and bubble diffusion. However, the ability of the sympathetic system to control HR is impaired and can lead to fatal consequences in some DCS cases.

At first glance, the post-DCS elevation of the parasympathetic modulation compared to baseline contradicts our 200-ft experiment, where both branches of the ANS were significantly depressed after neurological DCS (8). In that protocol, both neurological DCS symptoms and spinal cord injury were observed in most of the exposed swine. Because the efferent nerves of the ANS reside in the spinal cord, the observed spinal cord injury might explain the concurrent impairment of ANS function. However, in this experiment, no signs of neurological DCS or spinal cord injury were observed. As the ANS was intact, it actively regulated the cardiovascular system to protect against the detrimental effects of DCS. More importantly, the elevation of parasympathetic regulation occurred even before DCS was observed. As mentioned above, in a dive without DCS, the parasympathetic regulation immediately after surfacing should be higher than baseline, but less than that found while under pressure. However, in this study, after surfacing but before DCS onset, the parasympathetic regulation was not only greater than baseline, but also greater than its value during hyperbaric exposure. This implies that an abnormal elevation of the parasympathetic regulation compared to during hyperbaric exposure may portend impending DCS. Indeed, immediately after surfacing, but prior to DCS onset, an elevation of the parasympathetic regulation compared to the hyperbaric bottom stage was observed in all the parasympathetic parameters we measured: RMSSD, HF and the parasympathetic dynamics. If we examine these parameters in each of the 5 min segments, the increased parasympathetic parameters occur immediately upon reaching surface and much earlier than DCS onset (Table 8). Thus, it is possible that tracking the parasympathetic system dynamics could potentially serve as a noninvasive predictive measure for non-neurological DCS.

It should be noted, however, that while we can predict the onset of cutis and CP DCS, this approach cannot distinguish between them based on the elevated parasympathetic dynamics. Distinguishing between the two may be difficult due to their simultaneous onset in 6/9 swine as reported by the observers. Future studies with a larger set of animals are needed to sort out this interesting question. One additional point of note, most of the swine in this study began sleeping 30-120 min after reaching bottom; these were excluded from the statistical analyses because sleep is dominated by the parasympathetic activity (7). Finally, for a future study, a control group without DCS will be needed to calculate the specificity of the DCS prediction with the PDM. However, we believe the control data (without DCS) will have similar ANS dynamics as those represented during the baseline condition, thus, we expect a very good specific value with PDM.

In summary, dominance of the parasympathetic modulation was found in both hyperbaric chamber and SCUBA diving conditions. And more stresses were present in real dives, compared to simulation dives in chamber. PDM method has proved its capacity in monitoring the ANS alterations under different hyperbaric environments. In swine DCS model, we found neurological DCS and CP DCS resulted in different modulations in the ANS. The parasympathetic dynamics of PDM showed good sensitivity in prediction of CP DCS, which is the greatest finding in this study.

Future Studies

In this study, tracking the parasympathetic dynamics seems to be a promising method to detect the onset of cardiopulmonary DCS. And our PDM algorithm is more sensitive to DCS than traditional HRV analysis method. However, a control study where DCS is not induces is necessary to establish the real efficacy of PDM method. In such an experiment, elevation of the parasympathetic modulation will not be present post-dive, and we can calculate the specificity of PDM method for DCS prediction. Then a threshold for DCS detection can be determined through the plot of a receiver operating characteristic curve, where optimum sensitivity and specificity can be achieved.

Since the PDM method is very sensitive in DCS detection, it is probably also sensitive to other hyperbaric hazards, such as oxygen toxicity, nitrogen narcosis and high-pressure nervous syndrome. All these diseases exhibit dysfunction in nervous system (16). For example, nitrogen narcosis shows symptoms similar with the early stages of anesthesia (25). And our PDM method has shown its capability in discriminating between different concentration levels of anesthesia. Thus, it is potentially useful in diagnosis of high-pressure syndrome. Future studies using PDM to evaluate autonomic nervous activities during these hazards could benefit the diagnosis and prevention of these hyperbaric hazards.

References

1. http://en.wikipedia.org/wiki/Decompression_sickness. 2009].
2. Heart rate variability: standards of measurement, physiological interpretation and clinical use. Task Force of the European Society of Cardiology and the North American Society of Pacing and Electrophysiology. *Circulation* 93: 1043-1065, 1996.
3. Report on decompression sickness, diving fatalities and project dive exploration Durham: Divers Alert Network, 2005.
4. Report on decompression sickness, diving fatalities and project dive exploration Durham: Divers Alert Network, 2008.
5. **Arness MK**. Scuba decompression illness and diving fatalities in an overseas military community. *Aviat Space Environ Med* 68: 325-333, 1997.
6. **Atkins CE, Lehner CE, Beck KA, Dubielzig RR, Nordheim EV, and Lanphier EH**. Experimental respiratory decompression sickness in sheep. *J Appl Physiol* 65: 1163-1171, 1988.
7. **Baharav A, Kotagal S, Gibbons V, Rubin BK, Pratt G, Karin J, and Akselrod S**. Fluctuations in autonomic nervous activity during sleep displayed by power spectrum analysis of heart rate variability. *Neurology* 45: 1183-1187, 1995.
8. **Bai Y, Mahon RT, White JC, Brink PR, and Chon KH**. Impairment of the autonomic nervous function during decompression sickness in swine. *J Appl Physiol* 106: 1004-1009, 2009.
9. **Bain SA, Ting J, Simeonovic CJ, and Wilson JD**. Technique of venous catheterization for sequential blood sampling from the pig. *J Invest Surg* 4: 103-107, 1991.
10. **Broome JR, and Dick EJ, Jr.** Neurological decompression illness in swine. *Aviat Space Environ Med* 67: 207-213, 1996.
11. **Buttolph TB, Dick EJ, Jr., Toner CB, Broome JR, Williams R, Kang YH, and Wilt NL**. Cutaneous lesions in swine after decompression: histopathology and ultrastructure. *Undersea Hyperb Med* 25: 115-121, 1998.
12. **Carmichael K**. Scuba Diving - Physiology and Common Medical Conditions http://physiotherapy.curtin.edu.au/resources/educational-resources/exphys/00/scuba.cfm. [December, 4, 2008.
13. **Catron PW, Flynn ET, Jr., Yaffe L, Bradley ME, Thomas LB, Hinman D, Survanshi S, Johnson JT, and Harrington J**. Morphological and physiological responses of the lungs of dogs to acute decompression. *J Appl Physiol* 57: 467-474, 1984.
14. **Chon KH, Zhao H, Zou R, and Ju K**. Multiple time-varying dynamic analysis using multiple sets of basis functions. *IEEE Trans Biomed Eng* 52: 956-960, 2005.
15. **Chouchou F, Pichot V, Garet M, Barthelemy JC, and Roche F**. Dominance in cardiac parasympathetic activity during real recreational SCUBA diving. *Eur J Appl Physiol* 106: 345-352, 2009.
16. **Dean JB, Mulkey DK, Garcia AJ, 3rd, Putnam RW, and Henderson RA, 3rd**. Neuronal sensitivity to hyperoxia, hypercapnia, and inert gases at hyperbaric pressures. *J Appl Physiol* 95: 883-909, 2003.
17. **Dromsky DM, Toner CB, Survanshi S, Fahlman A, Parker E, and Weathersby P**. Natural history of severe decompression sickness after rapid ascent from air saturation in a porcine model. *J Appl Physiol* 89: 791-798, 2000.

18. **Eckberg DL**. Sympathovagal balance: a critical appraisal. *Circulation* 96: 3224-3232, 1997.
19. **Flook V**. Physics and physiology in the hyperbaric environment. *Clin Phys Physiol Meas* 8: 197-230, 1987.
20. **Francis TJ, Pezeshkpour GH, Dutka AJ, Hallenbeck JM, and Flynn ET**. Is there a role for the autochthonous bubble in the pathogenesis of spinal cord decompression sickness? *J Neuropathol Exp Neurol* 47: 475-487, 1988.
21. **Gempp E, and Blatteau JE**. Risk factors and treatment outcome in scuba divers with spinal cord decompression sickness. *J Crit Care* 2009.
22. **Gooden BA**. Mechanism of the human diving response. *Integr Physiol Behav Sci* 29: 6-16, 1994.
23. **Gurney A, and Manoury B**. Two-pore potassium channels in the cardiovascular system. *Eur Biophys J* 38: 305-318, 2009.
24. **Hirayanagi K, Nakabayashi K, Okonogi K, and Ohiwa H**. Autonomic nervous activity and stress hormones induced by hyperbaric saturation diving. *Undersea Hyperb Med* 30: 47-55, 2003.
25. **Hobbs M**. Subjective and behavioural responses to nitrogen narcosis and alcohol. *Undersea Hyperb Med* 35: 175-184, 2008.
26. **Horner SM, Murphy CF, Coen B, Dick DJ, Harrison FG, Vespalcova Z, and Lab MJ**. Contribution to heart rate variability by mechanoelectric feedback. Stretch of the sinoatrial node reduces heart rate variability. *Circulation* 94: 1762-1767, 1996.
27. **Kleiger RE, Miller JP, Bigger JT, Jr., and Moss AJ**. Decreased heart rate variability and its association with increased mortality after acute myocardial infarction. *Am J Cardiol* 59: 256-262, 1987.
28. **Kurita A, Nagayoshi H, Okamoto Y, Takase B, Ishizuka T, and Oiwa H**. Effects of severe hyperbaric pressure on autonomic nerve functions. *Mil Med* 167: 934-938, 2002.
29. **Laguna P, Thakor NV, Caminal P, Jane R, Yoon HR, Bayes de Luna A, Marti V, and Guindo J**. New algorithm for QT interval analysis in 24-hour Holter ECG: performance and applications. *Med Biol Eng Comput* 28: 67-73, 1990.
30. **Levett DZ, and Millar IL**. Bubble trouble: a review of diving physiology and disease. *Postgrad Med J* 84: 571-578, 2008.
31. **Lund VE, Kentala E, Scheinin H, Klossner J, Helenius H, Sariola-Heinonen K, and Jalonen J**. Heart rate variability in healthy volunteers during normobaric and hyperbaric hyperoxia. *Acta Physiol Scand* 167: 29-35, 1999.
32. **Lund VE, Kentala E, Scheinin H, Klossner J, Sariola-Heinonen K, and Jalonen J**. Hyperbaric oxygen increases parasympathetic activity in professional divers. *Acta Physiol Scand* 170: 39-44, 2000.
33. **Mahon RT, Dainer HM, Gibellato MG, and Soutiere SE**. Short oxygen prebreathe periods reduce or prevent severe decompression sickness in a 70-kg swine saturation model. *J Appl Physiol* 106: 1459-1463, 2009.
34. **Mahon RT, Dainer HM, and Nelson JW**. Decompression sickness in a swine model: isobaric denitrogenation and perfluorocarbon at depth. *Aviat Space Environ Med* 77: 8-12, 2006.
35. **Malpas SC**. Neural influences on cardiovascular variability: possibilities and pitfalls. *Am J Physiol Heart Circ Physiol* 282: H6-20, 2002.

36. **Marmarelis VZ**. Identification of nonlinear biological systems using Laguerre expansions of kernels. *Ann Biomed Eng* 21: 573-589, 1993.
37. **McGowan CL, Swiston JS, Notarius CF, Mak S, Morris BL, Picton PE, Granton JT, and Floras JS**. Discordance between microneurographic and heart-rate spectral indices of sympathetic activity in pulmonary arterial hypertension. *Heart* 95: 754-758, 2009.
38. **Miwa C, Sugiyama Y, Mano T, Iwase S, and Matsukawa T**. Sympatho-vagal responses in humans to thermoneutral head-out water immersion. *Aviat Space Environ Med* 68: 1109-1114, 1997.
39. **Nakatsuka I, Ochiai R, and Takeda J**. Changes in heart rate variability in sevoflurane and nitrous oxide anesthesia: effects of respiration and depth of anesthesia. *J Clin Anesth* 14: 196-200, 2002.
40. **Newton HB**. Neurologic complications of scuba diving. *Am Fam Physician* 63: 2211-2218, 2001.
41. **Pagani M, Mazzuero G, Ferrari A, Liberati D, Cerutti S, Vaitl D, Tavazzi L, and Malliani A**. Sympathovagal interaction during mental stress. A study using spectral analysis of heart rate variability in healthy control subjects and patients with a prior myocardial infarction. *Circulation* 83: II43-51, 1991.
42. **Parker EC, Ball R, Tibbles PM, and Weathersby PK**. Escape from a disabled submarine: decompression sickness risk estimation. *Aviat Space Environ Med* 71: 109-114, 2000.
43. **Pincus SM, and Viscarello RR**. Approximate entropy: a regularity measure for fetal heart rate analysis. *Obstet Gynecol* 79: 249-255, 1992.
44. **Ricksten SE, and Thoren P**. Reflex inhibition of sympathetic activity during volume load in awake normotensive and spontaneously hypertensive rats. *Acta Physiol Scand* 110: 77-82, 1980.
45. **Ross A, and Steptoe A**. Attenuation of the diving reflex in man by mental stimulation. *J Physiol* 302: 387-393, 1980.
46. **Schipke JD, and Pelzer M**. Effect of immersion, submersion, and scuba diving on heart rate variability. *Br J Sports Med* 35: 174-180, 2001.
47. **Schroeder EB, Liao D, Chambless LE, Prineas RJ, Evans GW, and Heiss G**. Hypertension, blood pressure, and heart rate variability: the Atherosclerosis Risk in Communities (ARIC) study. *Hypertension* 42: 1106-1111, 2003.
48. **Seals DR, Johnson DG, and Fregosi RF**. Hyperoxia lowers sympathetic activity at rest but not during exercise in humans. *Am J Physiol* 260: R873-878, 1991.
49. **Shibata S, Iwasaki K, Ogawa Y, Kato J, and Ogawa S**. Cardiovascular neuroregulation during acute exposure to 40, 70, and 100% oxygen at sea level. *Aviat Space Environ Med* 76: 1105-1110, 2005.
50. **Shida KK, and Lin YC**. Contribution of environmental factors in development of hyperbaric bradycardia. *J Appl Physiol* 50: 731-735, 1981.
51. **Sica AL, Ruggiero DA, Zhao N, and Gootman PM**. Developmental changes in heart rate variability during exposure to prolonged hypercapnia in piglets. *Auton Neurosci* 100: 41-49, 2002.
52. **Sloan RP, Shapiro PA, Bagiella E, Bigger JT, Jr., Lo ES, and Gorman JM**. Relationships between circulating catecholamines and low frequency heart period

variability as indices of cardiac sympathetic activity during mental stress. *Psychosom Med* 58: 25-31, 1996.
53. **Spira A**. Diving and marine medicine review part II: diving diseases. *J Travel Med* 6: 180-198, 1999.
54. **Sramek P, Simeckova M, Jansky L, Savlikova J, and Vybiral S**. Human physiological responses to immersion into water of different temperatures. *Eur J Appl Physiol* 81: 436-442, 2000.
55. **Tetzlaff K, and Thorsen E**. Breathing at depth: physiologic and clinical aspects of diving while breathing compressed gas. *Clin Chest Med* 26: 355-380, v, 2005.
56. **Tibbles PM, and Edelsberg JS**. Hyperbaric-oxygen therapy. *N Engl J Med* 334: 1642-1648, 1996.
57. **Torti SR, Billinger M, and Schwerzmann M**. Risk of decompression illness among 230 divers in relation to the presence and size of patent foramen ovale. *ACC Current Journal Review* 13: 25-25, 2004.
58. **Tripathi LCK**. Respiration And Heart Rate Variability : A Review With Special Reference To Its Application In Aerospace Medicine. *Indian Journal of Aerospace Medicine* 48: 64-75, 2004.
59. **Yamauchi K, Tsutsui Y, Endo Y, Sagawa S, Yamazaki F, and Shiraki K**. Sympathetic nervous and hemodynamic responses to lower body negative pressure in hyperbaria in men. *Am J Physiol Regul Integr Comp Physiol* 282: R38-45, 2002.
60. **Yamazaki F, Shiraki K, Sagawa S, Endo Y, Torii R, Yamaguchi H, Mohri M, and Lin YC**. Assessment of cardiac autonomic nervous activities during heliox exposure at 24 atm abs. *Aviat Space Environ Med* 69: 643-646, 1998.
61. **Yamazaki F, Wada F, Nagaya K, Torii R, Endo Y, Sagawa S, Yamaguchi H, Mohri M, Lin YC, and Shiraki K**. Autonomic mechanisms of bradycardia during nitrox exposure at 3 atmospheres absolute in humans. *Aviat Space Environ Med* 74: 643-648, 2003.
62. **Zhong Y, Wang H, Ju KH, Jan KM, and Chon KH**. Nonlinear analysis of the separate contributions of autonomic nervous systems to heart rate variability using principal dynamic modes. *IEEE Trans Biomed Eng* 51: 255-262, 2004.
63. **Zhong YR, Jan KM, Ju KH, and Chon KH**. Quantifying cardiac sympathetic and parasympathetic nervous activities using principal dynamic modes analysis of heart rate variability. *Am J Physiol-Heart C* 291: H1475-H1483, 2006.